Systematics of Spontaneously Fissioning Isomers*

H. C. Britt, S. C. Burnett, B. H. Erkkila, J. E. Lynn,† and W. E. Stein
Los Alamos Scientific Laboratory, University of California, Los Alamos, New Mexico 87544
(Received 17 May 1971)

Excitation functions have been measured for the production of fission isomers by (α,xn) reactions for bombarding energies of 20–29 MeV and by $(d,2n)$, (d,p), and (d,pn) reactions for bombarding energies of 9–14 MeV. Excitation functions for (α,xn) reactions were measured for targets of ^{233}U, ^{234}U, ^{235}U, ^{236}U, ^{238}U, ^{237}Np, ^{239}Pu, ^{240}Pu, ^{242}Pu, and ^{244}Pu. Excitation functions for deuteron reactions were measured for targets of ^{235}U, ^{237}Np, ^{239}Pu, ^{240}Pu, ^{242}Pu, ^{244}Pu, and ^{243}Am. New or more accurate half-lives were determined for the following fission isomers: ^{235m}Pu, 30 ± 5 nsec; ^{238m}Pu, 6.5 ± 1 nsec; ^{240m}Pu, 3.8 ± 0.3 nsec; ^{241m}Cm, 15.3 ± 1 nsec; and ^{245m}Cm, 23 ± 5 nsec. Isomers in ^{242}Cm and ^{244}Cm were identified but their half-lives were too long for measurement with the present techniques. The results are analyzed with a statistical model using realistic level-density expressions with many parameters fixed by comparison with experimental measurements of neutron-fission cross sections, neutron-to-fission decay widths, spallation cross sections, and fission lifetimes. This model is applied to the presently measured excitation functions and the results obtained previously by other groups for $(n,2n)$, $(p,2n)$, and (γ,n) reactions. With this model fission-barrier parameters are determined for Pu, Am, and Cm isotopes. Inconsistencies in the results obtained by applying this model to experimental isomer excitation functions indicate the directions for future refinements.

I. INTRODUCTION

The discovery of isomeric states in Am nuclei, which decayed by fission,[1] had relatively low spin values, and had excitation energies of ~3 MeV, was the first indication of the existence of shape isomers in actinide nuclei.[2] The theoretical prediction by Strutinski[3] of a secondary minimum in the potential-energy surface for certain actinide nuclei gave credibility to the concept of a shape isomer which could decay by fission. The discovery of gross structure in the subthreshold neutron-fission resonances for ^{237}Np[4] and ^{240}Pu[5] gave further support for this hypothesis.

Fission isomers have been produced by a wide variety of nuclear reactions and their properties studied by a variety of techniques. The reactions used to study the properties of fission isomers have included (n,γ),[6-10] $(n,2n)$,[11] $(p,2n)$,[12-14] $(d,2n)$,[12-14] (α,xn),[15-19] (γ,n),[20,21] and miscellaneous direct reactions such as (d,p), (d,t), and (d,pn).[12-14,22-24] These results give details on half-lives and production cross sections for various isotopes of U, Pu, Am, and Cm. In several cases[11-14,18,20,21] the experimental results included excitation functions for xn reactions that could be used to determine the excitation energy of the isomeric state above the ground state. These excitation functions were analyzed by the experimental groups using the simple model developed by Jackson[25] for the neutron-evaporation reactions leading to ground-state nuclei. Recently Jägare[26] has pointed out that this simple model is not really appropriate for the population of shape-isomeric states and has developed a more rigorous form of the Jackson model for this case. This model is an extension of a previous simplified statistical model suggested by Jungclaussen.[27]

In the present experiments excitation functions have been measured for the production of fission isomers by the bombardment of actinide targets with α-particle and deuteron beams. A list of the reactions studied is given in Table I. The results presented include those given in abbreviated form in an earlier letter.[18] The results of these experiments are analyzed with an improved statistical evaporation model and parameters of the fission barrier are determined for a series of Pu, Am, and Cm nuclei.

II. EXPERIMENTAL PROCEDURE

Delayed fragments were detected during the time between bursts of particles from the Los Alamos variable-energy cyclotron. The small cross sections for isomer production necessitated keeping the fission background due to scattered neutrons and γ rays to a minimum. We took advantage of the physical layout of the cyclotron building; instead of placing our fission chamber in the cyclotron experimental vault, the vault was used for steering, collimating, and focusing beams of α particles and deuterons (see Fig. 1). The fission chamber was mounted between the wall of the experimental vault and the building wall and a shielded beam dump was constructed outside the building; thus 1 m of concrete shielding lay between the chamber and both the collimating slits and the Faraday cup.

With careful collimation, focusing, and steering, stable beams of 50 to 500 nA were delivered through a maximum diameter of 1 cm in the target area. The stability and size of the beam were continuously monitored by observing the current deposited on an oversized Ta collimator ($\frac{1}{2}$-in. diam) placed in the fission chamber. The "scattered current" was always <1% of the beam current deposited at the Faraday cup. In order to eliminate the possibility of the beam striking the target holder, $\frac{3}{4}$-in.-diam target holders were used. Targets consisted of 100–400-μg/cm^2 deposits, vacuum-evaporated on carbon backings (the ^{244}Pu target was prepared by an electroplating process). All target material was enriched to >98% in the isotope of interest except for ^{235}U which was enriched to a purity of 93.2%.

TABLE I. Reactions studied, measured isomeric half-lives, and peak values of isomer-to-prompt-fission ratio.

Reaction	$T_{1/2}$ (nsec)	Peak isomer/prompt (units of 10^{-6})
^{232}Th(α, $2n$)^{234m}U	···	<0.2 [a]
^{233}U(α, $2n$)^{235m}Pu	30 ± 5	4.7
^{234}U(α, n)^{237m}Pu	100 ± 50	1.5 [b]
^{235}U(α, $2n$)^{237m}Pu	120 ± 50	19
^{236}U(α, n)^{239m}Pu	>50 [c]	1.8 [b]
^{236}U(α, $2n$)^{238m}Pu	6.5 ± 1.5	5
^{238}U(α, n)^{241m}Pu	>50 [c]	1.5 [b]
^{238}U(α, $2n$)^{240m}Pu	3.8 ± 0.3	130
^{238}U(α, $3n$)^{239m}Pu	>100 [c]	15
^{237}Np(α, n)^{240m}Am	>50 [c]	···
^{237}Np(α, $2n$)^{239m}Am	180^{+120}_{-60}	8.5
^{239}Pu(α, $2n$)^{241m}Cm	15.3 ± 1	2.3
^{240}Pu(α, $2n$)^{242m}Cm	>80 [c]	1.0
^{242}Pu(α, $2n$)^{244m}Cm	>100 [c]	2.8
^{242}Pu(α, $3n$)^{243m}Cm	>40 [c]	1.8
^{244}Pu(α, $2n$)^{246m}Cm	···	<2
^{244}Pu(α, $3n$)^{245m}Cm	23 ± 5	2.0
^{235}U(d, p)^{236m}U	>50 [c]	···
^{237}Np(d, $2n$)^{237m}Pu	120 [d]	20
^{239}Pu(d, pn)^{239m}Pu	>50 [c]	···
^{239}Pu(d, $2n$)^{239m}Am	>50 [c]	10
^{240}Pu(d, $2n$)^{240m}Am	>50 [c]	80
^{242}Pu(d, $2n$)^{242m}Am	>50 [c]	160
^{244}Pu(d, $2n$)^{244m}Am	>50 [c]	400
^{243}Am(d, p)^{244m}Am	>50 [c]	···
^{243}Am(d, pn)^{243m}Am	>50 [c]	···

[a] If $T_{1/2} > 20$ nsec.

[b] Average isomer/prompt ratio over region of measurements.

[c] Assumed $T_{1/2} = \infty$ in calculation of isomer cross section.

[d] Value assumed in calculating isomer cross sections.

The beam energy was measured by placing a gold scattering foil in the beam and detecting the scattered particles at 60° after they had been passed through a series of aluminum foils. The foils were adjusted to match the degraded energy of the particles with the energy of particles from a standard ^{239}Pu α source. The beam energy was then determined from range energy relations in Al.[28] In general, the energy of the cyclotron beam was measured to an over-all accuracy of ±0.2 MeV. This error includes both the natural width of the cyclotron beam, systematic error introduced due to uncertainty in the calibration of the energy monitor, and drifts in the energy during data accumulation. The full width at half maximum of the time distribution of the beam was approximately 3 nsec; a more significant parameter is the full width at 10^{-5} maximum which was measured to be 11 nsec.

The experimental setup was relatively simple. Because of the thickness of the target and backing, the recoiling compound nuclei formed in the interaction between the charged particles of the beam and target nuclei were trapped in the target. Most of the compound nuclei fissioned promptly but some evaporated neutrons and settled into shape-isomeric states. With two semiconductor detectors positioned ~3 cm from a target on either side of and perpendicular to the beam direction, both prompt- and isomeric-fission decays were observed. The detectors were totally depleted (125-μ deep), low-resistivity, p-n diffuse-junction detectors, 2 cm^2 in area and biased at greater than 150 V.

In order to increase both the rate of accumulation and the reliability of the data, the beam was allowed to traverse three targets in tandem, each viewed with two detectors (see insert of Fig. 1 and top of Fig. 2). Each fission detector provided a fast-timing signal which was shaped, amplified, and delayed; these signals were fed by pairs to the appropriate one of three coincidence units. Fission events were identified by a coincidence between those fragment pulses which exceeded a lower bound set to discriminate against scattered beam particles. The output of the coincidence unit was scaled and fanned; one of the fanned signals provided the tag identifying the target and detector pair in which the fission event occurred (A, B, or C of Fig. 2). The other fanned signal from the coincidence unit was fed to the start of a time-to-pulse-height converter; the stop pulse was supplied from the cyclotron oscillator.

Thus prompt and delayed isomeric fissions were identified by the time relationship between coincident fragment pulses and a signal from the cyclo-

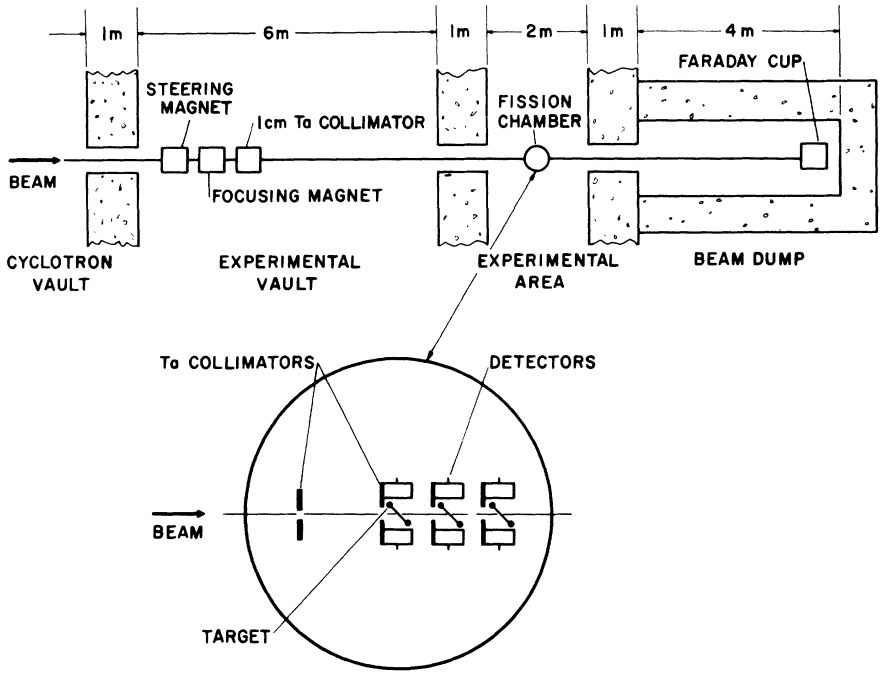

FIG. 1. Schematic diagram of the experimental layout for the fission-isomer experiments.

tron oscillator. The time information, identified as to origin, was analyzed and stored in 256 channels for each target and detector pair.

The present experimental setup could detect isomeric lifetimes greater than 3 nsec; above 150 nsec an accurate lifetime determination was not possible because of the ~80-nsec repetition rate of the cyclotron although the total number of isomeric decays was observable. Typical accumulated spectra are sketched at the base of Fig. 2. In part A of Fig. 2, the prompt-fission peak is shown at the right and the decay of a relatively long-lived isomer trails to the left; in part B, the decay of a relatively short state is seen to the left of the prompt peak. In part C, a time spectrum for a compound nucleus which apparently has no isomeric fission decay is shown, and only the prompt-fission peak is seen. An example of such a compound nucleus is that formed in the α bombardment of ^{232}Th or deuteron bombardment of ^{233}U or ^{234}U. Thus a ^{232}Th sample in one of the target positions provided simultaneous monitoring of the prompt-fission time spectrum and a check on the fission background occurring between beam bursts for α-particle experiments. For deuteron bombardments ^{233}U or ^{234}U targets were used for background.

Data analysis can best be discussed by examining a specific example: the 24.6-MeV α bombardment of a ^{238}U target. ^{242}Pu is the excited compound nucleus formed and it decays primarily in two ways; the nucleus may fission promptly or evaporate one or two neutrons with prompt fission competing at each stage. In the present experiment all prompt fissions are observed as coincident with the beam pulse. With very low probability the nucleus may decay to a shape-isomeric state after evaporating one or two neutrons, and then fission. The isomeric states are ^{240m}Pu and ^{241m}Pu, which decay with half-lives $T_1 = 3.8$ nsec and $T_2 > 100$ nsec, respectively.

The data for these decays are shown in Fig. 3 (circles). Simultaneous to the α bombardment of ^{238}U, a target of ^{232}Th was bombarded (triangles in Fig. 3); the total prompt fissions in ^{232}Th(α, f) were normalized to the total prompt fissions in ^{238}U(α, f). Accordingly the contribution of prompt fissions which occur in the tail of the beam pulse, and the fission background occurring between beam bursts can be estimated and the proper correction made.

In part (b) of Fig. 3, the corrected decay curve for the sum of ^{238}U$(\alpha, 2n)^{240m}$Pu and ^{238}U$(\alpha, n)^{241m}$Pu is shown. A least-squares routine was used to fit the circles to the sum of two exponential functions with characteristic decay lifetimes of 3.8 and ∞ nsec (in the present experiment, lifetimes >100 nsec can be adequately represented by ∞). Decay results for all of the targets investigated could be represented by fits to one or two components.

An additional correction to the data was necessary when targets of $^{240, 242, 244}$Pu were used. The

spontaneous fission rate for these targets was determined prior to and after each experimental run, and suitable corrections were made to the data.

III. RESULTS

A. Isomer Half-Lives

The isomer half-lives obtained in these experiments are listed in Table I. Because of the ~80-nsec repetition of the cyclotron beam pulses and the finite width of the beam pulses, meaningful half-life determinations could be made only for cases where 2 nsec $< T_{1/2} <$ 100 nsec. A review of half-life determinations by various authors has recently been given by Polikanov and Sletten.[14]

Typical decay curves for α-particle bombardment of uranium targets are shown in Fig. 4. For the ^{233}U$(\alpha, 2n)^{235m}$Pu the measured half-life, $T_{1/2} = 30 \pm 5$ nsec, is in reasonable agreement with the previous value[16] of $20 \pm (30\%)$ nsec measured by recoil techniques. A comparison with cross sections for the ^{237}Np$(p, 2n)^{236m}$Pu reaction indicates that the ^{234}U results are dominated by the ^{234}U$(\alpha, n)^{237m}$Pu reaction and the value $T_{1/2} = 100 \pm 50$ nsec is consistent with this conclusion. For the ^{235}U$(\alpha, 2n)^{237m}$Pu reaction the apparent half-life, $T_{1/2} = 120 \pm 50$ nsec, is consistent with a two-component decay with $T^1_{1/2} = 82$ nsec and $T^2_{1/2} = 1120$ nsec reported by Russo *et al.*[19] For ^{236}U two reactions are observed, ^{236}U$(\alpha, 2n)^{238m}$Pu and ^{236}U$(\alpha, n)^{239m}$Pu. For ^{238m}Pu a value of $T_{1/2} = 6.5 \pm 1$ nsec is determined. At 24.6 MeV the ^{238}U results contain two components, ^{238}U$(\alpha, 2n)^{240m}$Pu with $T_{1/2} = 3.8 \pm 0.3$ nsec and ^{238}U$(\alpha, n)^{241m}$Pu where $T_{1/2} = \infty$ was as-

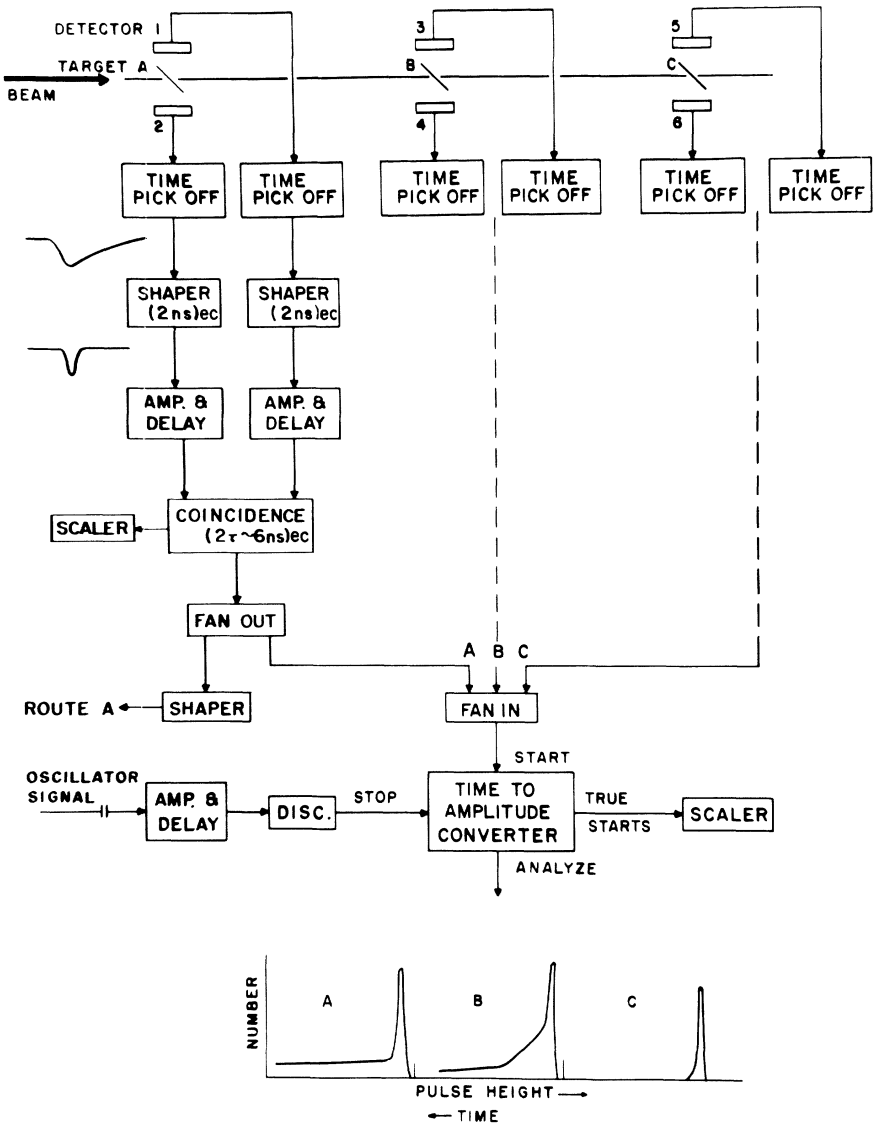

FIG. 2. Block diagram of the electronics setup.

sumed. At higher energies the reaction $^{238}U(\alpha, 3n)$-^{239m}Pu with an assumed $T_{1/2} = \infty$ becomes dominant. The value $T_{1/2} = 3.8 \pm 0.3$ nsec is in reasonable agreement with the value of 4.4 ± 0.8 nsec reported by Vandenbosch and Wolf.[15]

Typical decay curves for α-particle bombardment of Np and Pu isotopes are shown in Fig. 5. For $^{237}Np(\alpha, 2n)^{239m}Am$ the value $T_{1/2} \sim 180$ nsec is in good agreement with $T_{1/2} = 160 \pm 40$ nsec from Lark *et al.*[13] The reaction $^{239}Pu(\alpha, 2n)^{241m}Cm$ gives a value $T_{1/2} = 15.3 \pm 1$ nsec which is a better determination than the values 19[14] and 20 nsec[16] previously reported. The lifetimes are too long and cross sections too low for a determination of the half-lives of isomers formed by bombardments of ^{240}Pu and ^{242}Pu, but the present measurements do indicate the existence of fission isomers in ^{242}Cm and ^{244}Cm. Half-lives for these isomers have been determined[16] as 180 ± 70 nsec and ≥ 500 nsec for ^{242m}Cm and ^{244m}Cm, respectively. The reaction $^{244}Pu(\alpha, 3n)^{245m}Cm$ yields a new isomer with $T_{1/2} = 23 \pm 5$ nsec. A more recent measurement of this reaction by Wolf and Unik[29] yields a more accurate value of 15 ± 3 nsec for the isomer in ^{245}Cm, and Metag *et al.*[16] have obtained a value of 12 nsec for this isomer.

For the deuteron bombardments all the isomers have lifetimes too long to be determined with the present techniques and in most cases half-lives have been previously determined by other techniques.[14]

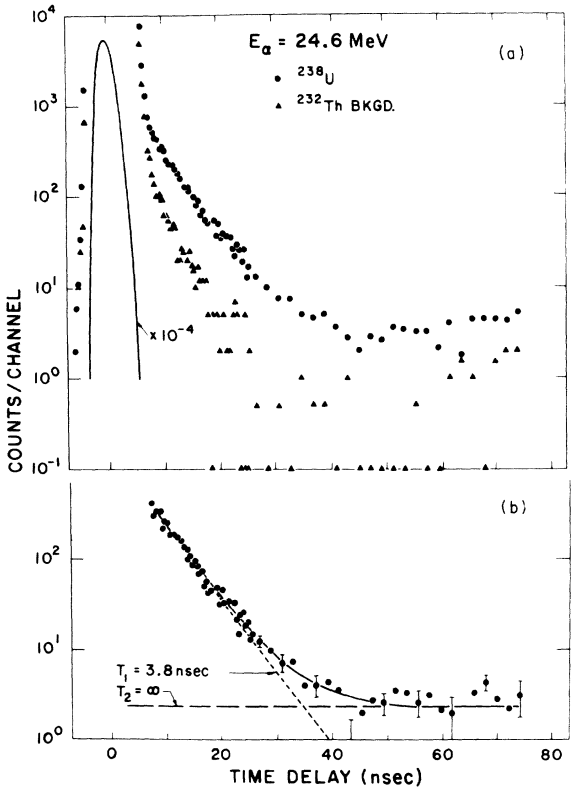

FIG. 3. Representative data obtained for the $^4He + ^{238}U$ reaction showing background as measured by the $^4He + ^{232}Th$ reaction. Points in part (b) have been corrected for background, and the solid line is a least-squares fit to the data assuming a two-component decay with half-lives of 3.8 nsec and ∞.

B. Excitation Functions (α Particles)

The isomer excitation functions obtained from the α-particle bombardments are shown in Figs. 6 and 7. In Figs. 6 and 7 the points indicated by solid circles represent cases where isomeric half-lives were measured and the solid squares are cases where the half-lives are too long for measurements using the present techniques. In many cases there is more than one half-life component contributing to the isomeric fission at some bombarding energies. For the ^{236}U, ^{238}U, and ^{239}Pu targets the two components can be separated uniquely because of the difference in half-lives. For ^{235}U, ^{237}Np, ^{242}Pu, and ^{244}Pu the two components are separated by extrapolating the measured isomer/prompt ratios to higher energies. In principle it should have been possible to separate the two components in the ^{244}Pu bombardment but in practice the statistical accuracies at a given energy were too poor to allow a unique separation.

For specific targets the following comments are applicable:

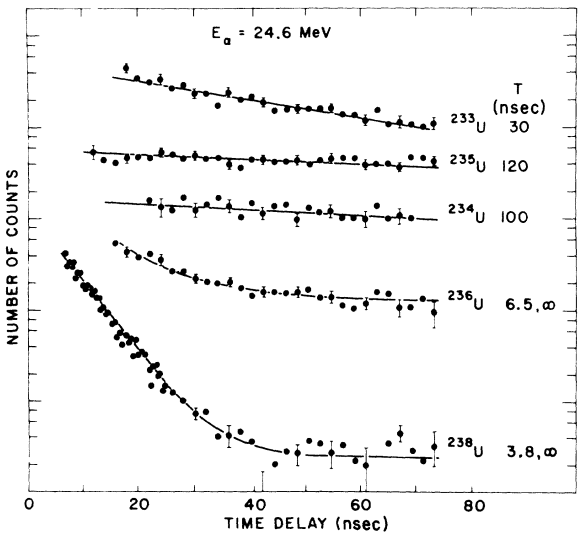

FIG. 4. Representative decay curves for fission isomers resulting from the bombardment of uranium targets by ^4He particles. Solid lines represent least-squares fits with the half-lives indicated on the figure.

^{236}U and ^{238}U. The data indicate contributions from both (α,n) and $(\alpha,2n)$ reactions and at higher energies the $(\alpha,3n)$ reaction dominates in the ^{238}U measurements.

^{234}U. The $^{237}Np(p,2n)^{236m}Pu$ data of Lark *et al.*[13] indicate a peak isomer/prompt ratio of $\sim 4\times10^{-7}$. The measured isomer/prompt ratio of $\sim 10^{-6}$ for the ^{234}U results suggests that these results are dominated by the (α,n) reaction.

^{237}Np, ^{242}Pu and ^{244}Pu. For ^{237}Np the tail of the (α,n) component must be subtracted from the $(\alpha,2n)$ results by extrapolating the low-energy behavior. A similar situation occurs with the tail of the $(\alpha,2n)$ and rise of $(\alpha,3n)$ for the ^{242}Pu and ^{244}Pu results.

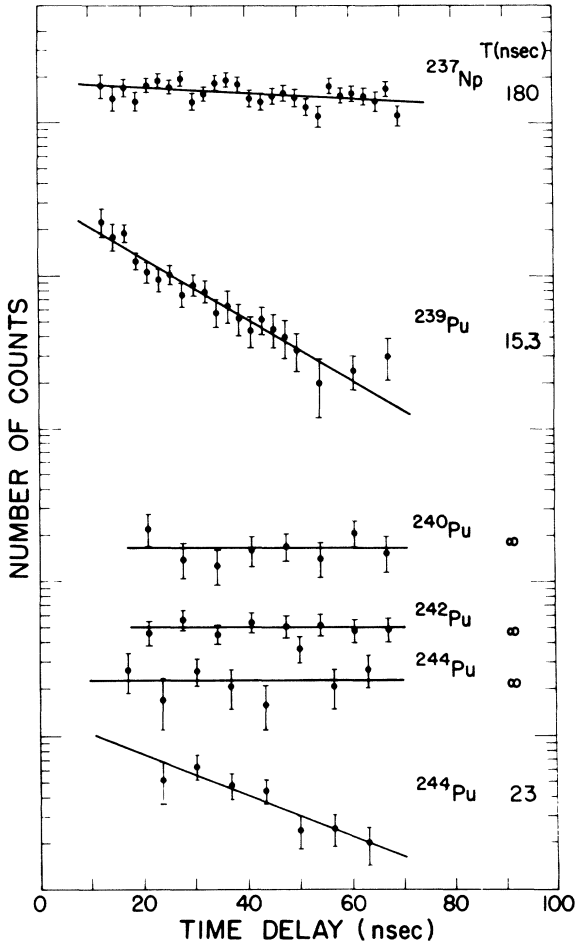

FIG. 5. Representative decay curves for fission isomers resulting from the bombardment of ^{237}Np and various plutonium targets. Solid lines represent least-squares fits with the half-lives indicated on the figure. The results for ^{240}Pu and ^{242}Pu are summed over all energies. For ^{244}Pu the $T_{1/2}=\infty$ component is obtained from data taken at $E_\alpha \sim 25$ MeV and the $T_{1/2}=23$-nsec component from the data taken at $E_\alpha = 28$–29 MeV.

^{234}U, ^{239}Pu, and possibly also ^{240}Pu. The low-energy tail results from a background due to neutron fission of the target nuclei. This conclusion was verified for the ^{239}Pu target by making measurements with the target adjacent to, but not directly in, the α-particle beam. The dependence indicated by the solid line for the ^{239}Pu isomer/prompt results corresponds to an approximately constant equivalent background cross section of ~ 0.05 μb. The effective background cross section at ~ 21 MeV for ^{235}U is also ~ 0.05 μb. Thus, these results suggest that the lower limit of sensitivity for present techniques is ~ 0.05 μb.

C. Excitation Functions (Deuterons)

Excitation functions for isomer production from deuteron bombardment of ^{235}U, ^{239}Pu, and ^{243}Am are shown in Figs. 8 and 9.

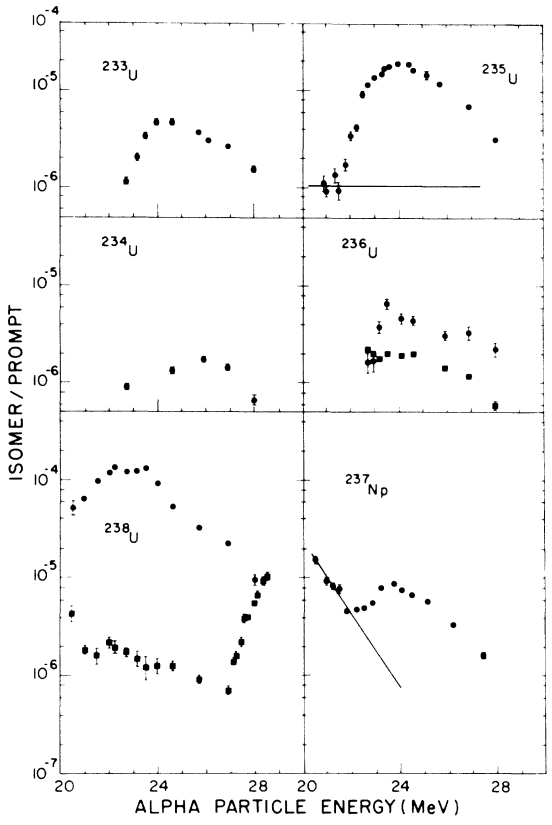

FIG. 6. Excitation functions for fission-isomer production from ^{4}He bombardment of ^{237}Np and uranium targets. Solid circles indicate cases for which half-lives were determined and solid squares, cross sections for which it was assumed $T_{1/2}=\infty$. The solid line on the ^{237}Np results represents an estimate of the contribution from the (α,n) reaction. The solid line on the ^{235}U results represents an estimate of the contribution from neutron background reactions.

For the ^{235}U bombardments isomers are formed only by the (d,p) reaction and for ^{243}Am at the lowest energies the isomer production should be dominated by the (d,p) reaction [the ^{243}Am$(d,2n)^{243m}$Cm reaction should have a peak isomer/prompt ratio of $\sim 1-2\times10^{-6}$]. A comparison of the ^{235}U$(d,p)^{236m}$U and ^{243}Am$(d,p)^{244m}$Am reactions indicates that the isomer-production rates for these two targets are essentially identical.

For ^{240}Pu$(d,p)^{241m}$Pu and ^{242}Pu$(d,p)^{243m}$Pu isomer/prompt ratios were obtained at $E_d = 8.85$ MeV by fitting the experimental results to two components: $T_{1/2} = \infty$ for $(d,2n)$ reaction, and $T_{1/2} = 30$ nsec for ^{241m}Pu; or $T_{1/2} = 33$ nsec [14] for ^{243m}Pu. From a least-squares fit the relative contributions from short and long half-life components could be roughly determined for known half-lives. However, the data were not of sufficient accuracy to determine meaningful half-lives for the two components. In the ^{240}Pu case the results are consistent with the presence of a 30-nsec component but do not strongly confirm its existence or half-life.[14] The total isomer cross section for ^{240}Pu$(d,p)^{241m}$Pu was taken as 2.7 times the cross section for the 30-nsec component to allow for the fraction going to the 27-μsec component.[14] These results along with previous measurements[13,14] show that the (d,p) isomer/prompt ratios for ^{240}Pu and ^{242}Pu targets are similar to those observed for ^{235}U and ^{243}Am. The dashed lines in Fig. 8 show the limits assumed for the correction to ^{240}Pu, ^{242}Pu, and ^{244}Pu results for the (d,p) contribution to the total isomer cross section. For the ^{239}Pu target the ^{239}Pu$(d,p)^{240m}$Pu reaction does not contribute to the total measured cross section because of the short half-life (3.8 nsec) for ^{240m}Pu.

At energies near 14 MeV the deuteron reactions on ^{243}Am and ^{239}Pu are dominated by the (d,pn) reaction and Fig. 9 shows that the isomer/prompt ratios are similar for the two targets. The solid line in Fig. 9 is the assumed shape for the (d,pn) isomer ratio used to correct the ^{239}Pu data to obtain the isomer/prompt ratios for the ^{239}Pu$(d,2n)$-^{239m}Am reaction. The shape for the ^{239}Pu(d,pn) isomer/prompt excitation function was taken from the the results of Polikanov and Sletten[14] but the absolute cross section indicated by the present results

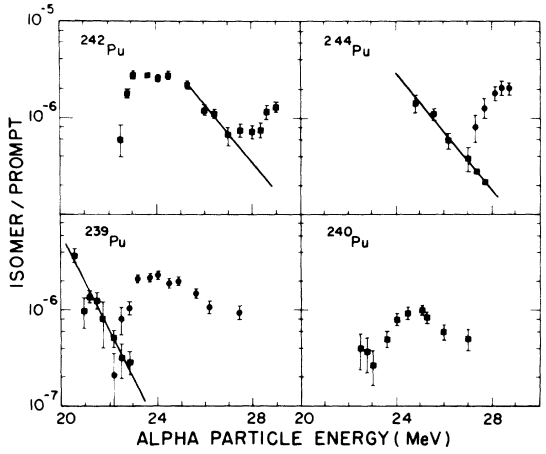

FIG. 7. Excitation functions for fission-isomer production from ^{4}He bombardment of plutonium targets. Solid circles indicate cases for which half-lives were determined and solid squares, cross sections for which it was assumed $T_{1/2} = \infty$. The solid line on the ^{239}Pu results represents an estimate of the contribution from neutron background reactions. The solid lines on the ^{242}Pu and ^{244}Pu results represent estimates of the cross section for $(\alpha,2n)$ reactions.

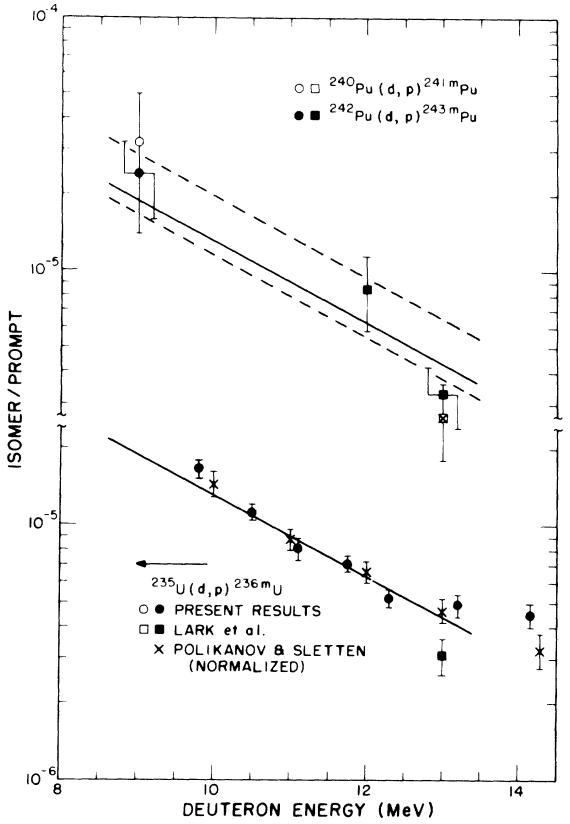

FIG. 8. Excitation functions for (d,p) reactions on ^{235}U, ^{240}Pu, and ^{242}Pu. The points at 8.85 MeV on ^{240}Pu and ^{242}Pu were obtained by fitting the experimental results to two half-life components as described in the text. The ^{235}U$(d,p)^{236m}$U data of Polikanov and Sletten (Ref. 14) have been arbitrarily normalized to give the best agreement with present measurements. Squares represent results taken from Lark *et al.* (Ref. 13). The solid line on the plutonium results is a line drawn by eye through the ^{235}U$(d,p)^{236m}$U results. The dotted lines represent limits for the corrections applied to data from deuteron bombardments of plutonium targets for the (d,p) contribution to the total isomer production.

is approximately 3 times greater than the value previously reported.[14]

The total isomer-prompt excitation functions for deuteron bombardment of ^{237}Np and Pu targets are shown in Fig. 10. The observed isomers are produced primarily by $(d, 2n)$ reactions with small but significant contributions from the (d, pn) reaction for ^{239}Pu and from (d, p) reactions for ^{240}Pu, ^{242}Pu, and ^{244}Pu. In results shown later in this paper the observed isomer cross sections have been corrected for (d, p) and (d, pn) contributions to obtain estimated cross sections for the $(d, 2n)$ reaction alone.

D. Comparison of Results from Various Experiments

For xn evaporation reactions to form fission isomers it is expected that the method of formation of the original compound nucleus should not strongly influence the isomer-to-prompt-fission ratios. To check this assumption comparisons have been made of the isomer/prompt ratios for $(p, 2n)$, $(d, 2n)$, $(\alpha, 2n)$, and $(n, 2n)$ reactions leading to the same fission isomers. Results of these comparisons are shown in Figs. 11 and 12 for fission isomers ^{237m}Pu, ^{239m}Am, ^{240m}Am, and ^{242m}Am. The results are converted to a consistent energy scale, $E^* - B_{2n}$, using the nuclear-mass systematics of Wapstra, Kurzeck, and Anisinoff.[30] Except for the $(n, 2n)$ results which will be discussed below there are no arbitrary normalization factors involved in these comparisons. The results in Figs. 11 and 12 show very good agreement between results obtained using different compound-nucleus reactions. These comparisons also show the good agreement between the present results obtained by direct counting techniques and results from the Copenhagen group[12, 13] using recoil techniques.

For ^{239m}Am there is a small apparent discrepancy between the $(\alpha, 2n)$ and $(p, 2n)$ results which could be due to either a 30% underestimate of the isomer/prompt ratio for the $(p, 2n)$ results[13] or an error of ~0.2 MeV in the absolute energy scale for the $(\alpha, 2n)$ measurements. In both cases, this magnitude error is roughly at the expected limit of error for the experiment. Also for ^{239m}Am the $(d, 2n)$ results give an isomer/prompt ratio about 25% greater than indicated from the $(\alpha, 2n)$ results. The most likely cause of this discrepancy is that

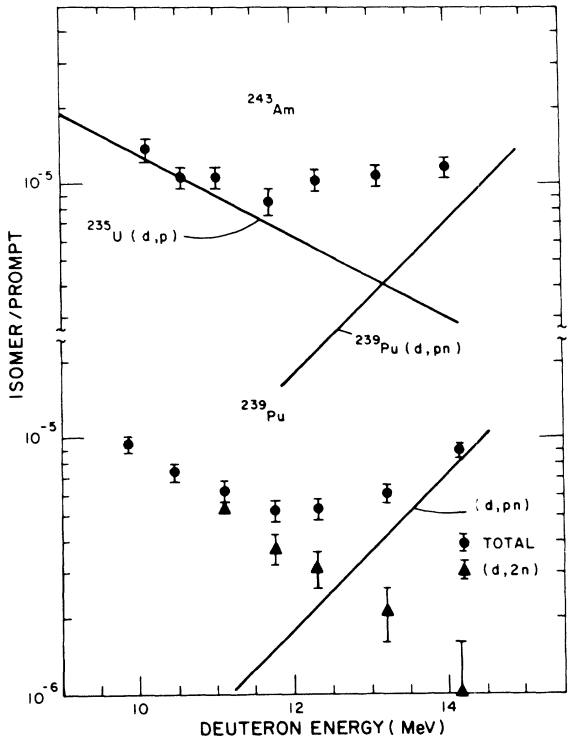

FIG. 9. Excitation functions for deuteron reactions on ^{239}Pu and ^{243}Am targets. For the ^{239}Pu the solid line represents the estimate of contributions from the (d, pn) reaction and the solid triangles represent estimates of the $(d, 2n)$ contributions obtained by subtracting the (d, pn) portion from the total cross section.

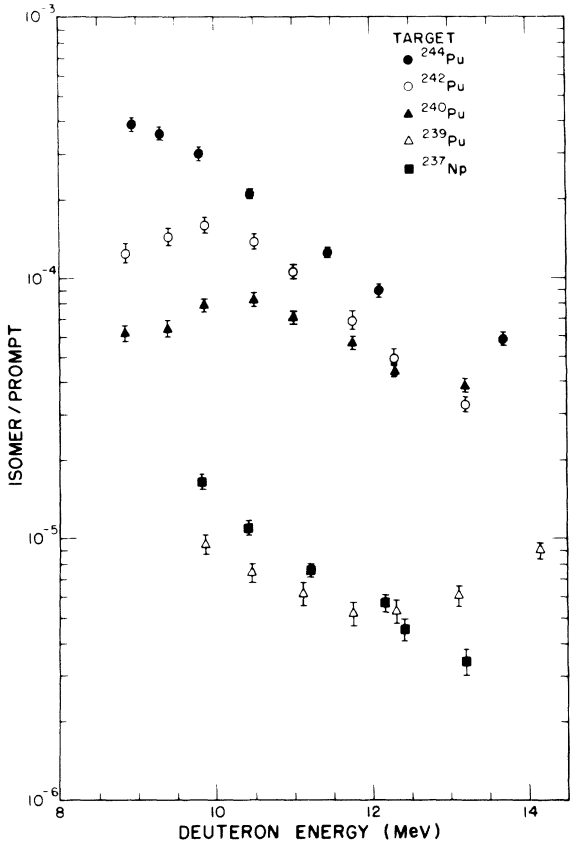

FIG. 10. Excitation functions for deuteron reactions on ^{237}Np and various plutonium targets.

there is a small contribution to the $(d, 2n)$ results from the (d, p) reaction which has not been properly taken into account. Alternatively this discrepancy could be due to an error in the $(\alpha, 2n)$ energy scale or to an error in the neutron binding energy for ^{241}Am which is not precisely known.[30] The very good correspondence between $(\alpha, 2n)$ and $(d, 2n)$ results for ^{237m}Pu makes it seem unlikely that the α-beam-energy measurements are systematically in error by more than ±0.2 MeV.

For ^{242}Am the measured isomer cross sections[11] were converted to isomer/prompt ratios assuming a constant compound-nucleus formation cross section of 1.0 b. This value is about $\frac{1}{2}$ the expected value and may indicate that the reported $(n, 2n)$ isomer cross sections are systematically low by about a factor of 2.

IV. STATISTICAL ANALYSIS OF ISOMER EXCITATION FUNCTIONS

A. Statistical Model for Isomer Production

A statistical model has been developed to calculate cross sections for the formation of fission isomers in neutron-evaporation reactions assuming a two-peaked fission barrier and standard methods for calculating the widths for various decay modes. The calculations are schematically illustrated in Fig. 13 and will be described in detail below. In the notation used A denotes the nucleus containing the observed isomer, $A+1$ the nucleus which feeds the isomeric state by neutron evaporation, and $A+2$ or $A+3$ are the compound nuclei formed in the original capture reaction.

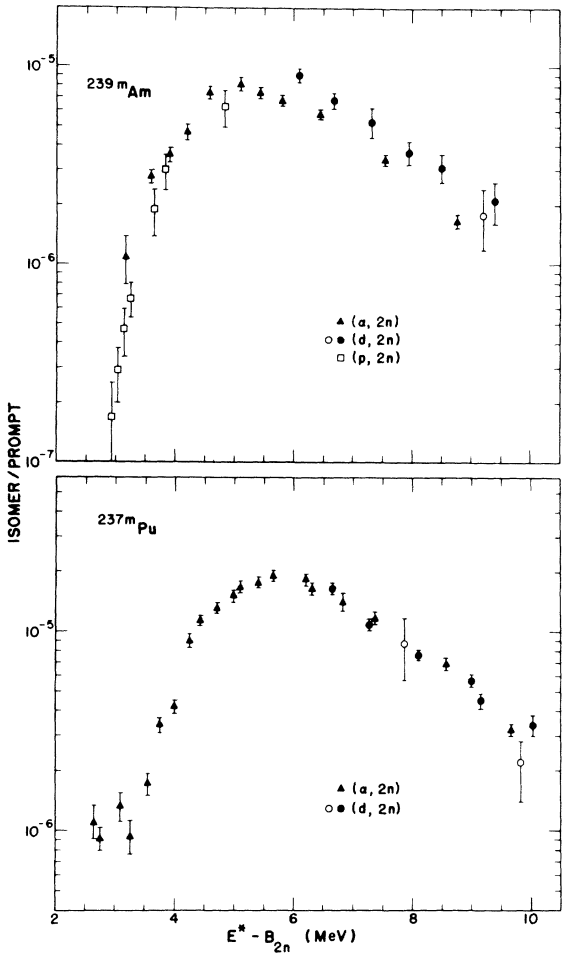

FIG. 11. Excitation functions from various reactions leading to fission isomers in ^{237}Pu and ^{239}Am. Solid points are data from the present experiment. Open points are taken from Lark *et al.* (Ref. 13).

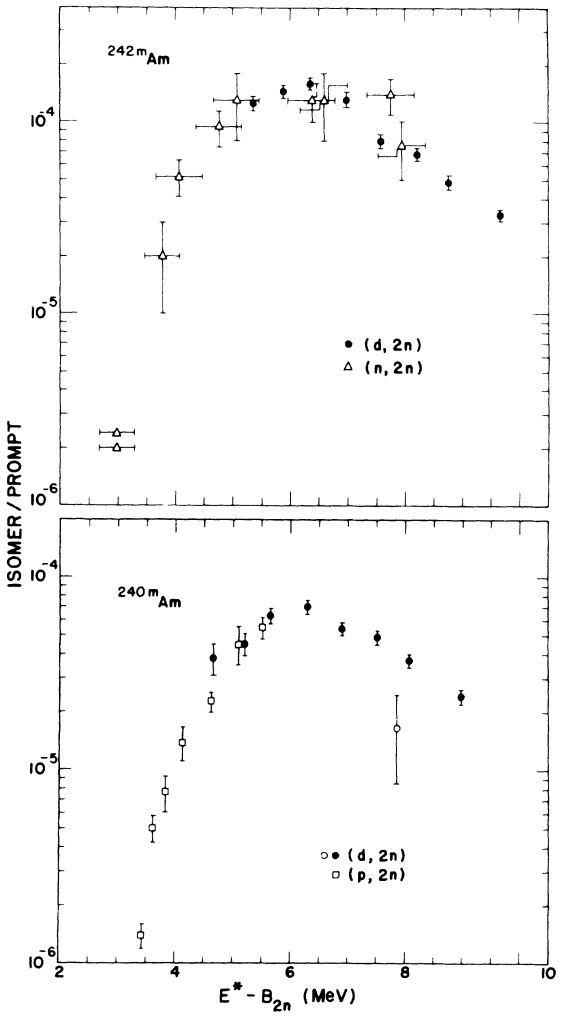

FIG. 12. Excitation functions from various reactions leading to fission isomers in ^{240}Am and ^{242}Am. Solid points are data from the present experiment. Open squares and circles are from Bjørnholm *et al.* (Ref. 12) and open triangles are from Flerov *et al.* (Ref. 11).

1. Population of $A+1$ Nucleus

The majority of the decays to the $A+1$ nucleus populate states in the first potential well and for purposes of calculating the population of isomers in the A nucleus the small fraction ($\sim 10^{-4}$) of nuclei decaying directly from the second well can be ignored. The fraction of nuclei which decay from the $A+2$ to $A+1$ nuclei by neutron emission is given by $\langle \Gamma_n/(\Gamma_n+\Gamma_f)\rangle_{A+2}$ where the ratio Γ_n/Γ_f is taken from the systematics[31] of Vandenbosch and Huizenga. For a $2n$ reaction the distribution of excitation energies in the $A+1$ nucleus can be satisfactorily approximated by a Maxwellian energy distribution for the emitted neutron,

$$N(\epsilon) \propto \epsilon e^{-\epsilon/T_e},$$

where $\epsilon = E^*_{\max}(A+1) - E^*(A+1)$ is the energy of the outgoing neutron and $E^*_{\max}(A+1) = E^*(A+2) - B_n(A+2)$ is the maximum excitation energy possible in the $A+1$ nucleus. A value $T_e = 0.6$ MeV was used in the $2n$ calculations which is a temperature appropriate for the average excitation-energy region populated by evaporation of the first neutron.

For the case of the formation of isomers by $3n$ reactions the fraction of nuclei decaying to the $A+1$ nucleus is given by $\langle \Gamma_n/(\Gamma_n+\Gamma_f)\rangle_{A+3} \times \langle \Gamma_n/(\Gamma_n+\Gamma_f)\rangle_{A+2}$ and the spectrum of excitations was obtained by folding together two Maxwellian distributions with $T_e(A+2) = 0.75$ MeV and $T_e(A+1) = 0.55$ MeV. These temperatures are appropriate for the average excitation energies populated by the first and second neutron evaporations, respectively.

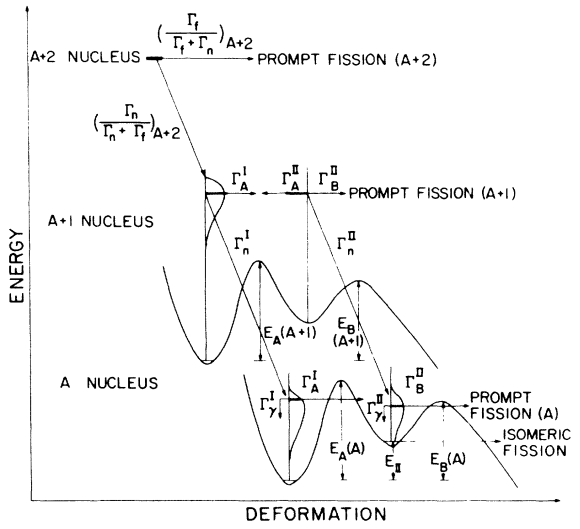

FIG. 13. A schematic drawing of the statistical model used to calculate fission-isomer cross sections for $(2n)$ evaporation reactions. Decays of the nucleus A to the nucleus $A-1$ by neutron emission were included in the calculations where energetically allowed.

2. Population of A Nucleus

For the relevant excitation energies the decay of the $A+1$ nucleus is dominated by fission and neutron emission. Neglecting γ-ray deexcitation the excited $A+1$ nucleus can decay by neutron emission to the nucleus A at either the normal (well I) or isomeric (well II) deformations or it can decay by prompt fission. In a strong-coupling approximation these decay modes are governed by the widths for penetrating the two peaks of the fission barrier $\Gamma^{\rm I}_A$, $\Gamma^{\rm II}_A$, and $\Gamma^{\rm II}_B$ and the neutron decay widths in the two equilibrium deformations, $\Gamma^{\rm I}_n$ and $\Gamma^{\rm II}_n$. For convenience in calculating the isomer cross sections the effective number of decay channels for a particular mode, $N = 2\pi\Gamma/D$, is used, where D is the level spacing in the appropriate well at the appropriate excitation energy. For the various decay modes

$$N_A = 2\pi\Gamma^{\rm I}_A/D_{\rm I} = 2\pi\Gamma^{\rm II}_A/D_{\rm II},$$

$$N_B = 2\pi\Gamma^{\rm II}_B/D_{\rm II},$$

$$N_{\rm I} = 2\pi\Gamma^{\rm I}_n/D_{\rm I}, \quad N_{\rm II} = 2\pi\Gamma^{\rm II}_n/D_{\rm II}.$$

If, as illustrated in Fig. 13, there is an initial population K of nuclei at some particular energy in well I in the $A+1$ nucleus, the number of nuclei decaying by the three modes is given by:
(a) decay to A nucleus in well I,

$$P_{\rm I} = KN_{\rm I}(N_A + N_{\rm II} + N_B)/\alpha,$$

where

$$\alpha = N_A(N_{\rm I} + N_{\rm II} + N_B) + N_{\rm I}(N_{\rm II} + N_B);$$

(b) decay to A nucleus in well II,

$$P_{\rm II} = KN_A N_{\rm II}/\alpha;$$

and (c) decay by prompt fission from $A+1$ nucleus,

$$P_f = KN_A N_B/\alpha.$$

These expressions are equivalent to expressions derived by Jägare[26] using a time-dependent decay formalism. In these calculations the relevant widths are calculated using standard considerations[32] and are discussed in more detail in Appendix A. The level-density expression used in these calculations was taken from Gilbert and Cameron.[33] The level-density expression was generalized by assuming the same form in wells I and II for the neutron (or γ-ray) decay widths with $a_n = a_{\rm I} = a_{\rm II}$ taken from experimental systematics[33] and assuming the same level-density parameter for the calculation of the transitions across the two peaks of the fission barrier, $a_f = a_A = a_B$. The ratio a_f/a_n was then determined by requiring that the calculated

widths reproduce experimental determinations of $\langle \Gamma_n/\Gamma_f \rangle$. Further details of the parameter determinations and the sensitivity of the calculations to various parameter changes are discussed in Appendix B.

3. *Decay of A Nucleus*

From the decay calculations for the $A+1$ nucleus the relative population of nuclei as a function of excitation energy in the two wells is determined. Then to determine the desired experimental quantities [relative cross sections to the ground state (well I), shape-isomeric state (well II), and prompt fission] the decay of the excited states in wells I and II must be considered. In this calculation the important quantities are the competition between γ-ray emission ($\Gamma_\gamma^{\mathrm{I}}$) and penetration of barrier A (Γ_A^{I}) or neutron emission to the nucleus $A-1$ [$\Gamma_n^{\mathrm{I}}(A)$] for states excited in the first potential well. In the second potential well the major competing decay modes (for cases where $E_A > E_B$) are γ-ray emission ($\Gamma_\gamma^{\mathrm{II}}$) and penetration of barrier B (Γ_B^{II}) leading to prompt fission. It is assumed that even below the height of barrier B there is strong coupling between the fission mode and the compound excitations so that the decay width Γ_B^{II} is governed only by the penetrability of barrier B and the D_{II} level spacing. Implications of this assumption are discussed in more detail in Appendix B.

In these calculations it is assumed that after the emission of a γ ray the nucleus is caught in one of the potential wells and will undergo further decay to the bottom (ground state or shape-isomeric state). This assumption is not appropriate for the decay of states well above the fission barrier where after emission of a prompt γ ray the nucleus may still have a large probability of decaying by fission. Since the contribution to the isomer population from high excitation energies is relatively small, the effect of γ-ray emission followed by fission was approximately taken into account by assuming that for $E^* < E_B + 1.0$ MeV all γ-ray decays of states in well II lead to population of the fission-isomeric state, and all decays for $E^* > E_B + 1.0$ MeV lead to fission or prompt neutron emission. This assumption has only a small effect on the calculations and the sensitivity of the calculations to this assumption is discussed in more detail in Appendix B.

In the high-energy part of the isomer excitation functions the major contribution to isomer formation comes from nuclei which are initially excited in the first well and then penetrate barrier A through to the second well and decay by γ-ray emission. This process is very dependent upon the degree of coupling between the class I states in the first well and the class II states in the isomeric well. In the present calculations this decay is considered a two-step process dependent on the product $\Gamma_A^{\mathrm{I}} \times \Gamma_\gamma^{\mathrm{II}}$ which is appropriate for the case where the class II levels are very broad. However, for the case where the class II levels are very narrow this two-step calculation gives a gross overestimate for the process and a more realistic calculation using first-order perturbation theory[32] gives a negligible contribution to isomer production from states excited in the first well. In the present case much of the region of interest occurs in the transition region between these two extremes. In the present model a simplifying assumption is made that above a critical excitation energy the two-step approximation is valid and below this energy the first-order perturbation theory results are appropriate. In comparisons to experimental results it was assumed that the critical excitation energy corresponded to the energy at which $\Gamma_{\mathrm{total}}^{\mathrm{II}} = D_{\mathrm{I}}$. The sensitivity of the calculated isomer excitation functions to this assumption and to the value used for the critical excitation energy is discussed in more detail in Appendix B.

B. Applications of Model to Experimental Results

Using the model described in the previous section the ratio of isomeric-to-prompt-fission cross sections can be calculated as a function of the initial excitation energy for $2n$ and $3n$ evaporation reactions. In order to obtain the most reliable fission-barrier parameters and/or provide the best test of this statistical model it is advantageous to specify as many parameters as possible from outside sources. The sensitivity of the calculations to various parameters is discussed in detail in Appendix B. A brief outline of the considerations used in fixing some of the model parameters and a discussion of the parameters left to be determined by comparison to fission-isomer excitation functions are given below.

The relative competition between neutron emission and the penetration of barrier A leading to fission is dependent on the parameters E_A and the ratio of level-density parameters a_f/a_n. For certain odd-neutron nuclei the larger of the two fission barriers can approximately be determined from measured neutron-fission thresholds or equivalent fission thresholds determined from (d,pf) or (t,pf) reactions. From fits to isomer cross sections discussed below it is found that for the Pu, Am, and Cm isotopes of interest the first barrier is higher and, therefore, measured fission thresholds can be equated with E_A. Experimental fission-threshold measurements for odd-neutron compound nuclei indicate values[34,35] of $E_A \sim 5.8$, 5.8, 5.5 MeV

for ^{241}Pu, ^{243}Pu, ^{245}Pu, values[36,37] of $E_A \sim 6.4$, 6.3 MeV for ^{242}Am, ^{244}Am; and values[38] of $E_A \sim 6.3$, 6.1, 5.6 for ^{245}Cm, ^{247}Cm, ^{249}Cm. Unfortunately, most of the nuclei involved in the fission-isomer reactions are lighter than those for which threshold measurements are available. For lack of more detailed information isomer calculations were performed assuming that E_A does not depend on A and has values 5.8 MeV for Pu isotopes, 6.4 MeV for Am isotopes, and 6.2 MeV for Cm isotopes. This assumption appears reasonable for the Pu and Am isotopes but may not be as well justified for Cm isotopes. After E_A was fixed, the ratio a_f/a_n could be determined by comparison with experimental $\langle \Gamma_n/\Gamma_f \rangle$ measurements (Appendix B).

The isomer cross sections are not very sensitive to the curvatures of the two barriers but for ^{240}Pu these curvatures can be estimated by comparison with experimental half-lives for spontaneous fission from the ground and shape-isomeric states. For $E_A = 5.80$ MeV, $\hbar\omega_A = 1.30$ MeV; $E_{II} = 2.60$ MeV, $\hbar\omega_{II} = 1.00$ MeV; and $E_B = 5.30$ MeV, $\hbar\omega_B = 0.60$ MeV, lifetime calculations[39] give $T_{1/2}^{SF} = 0.8 \times 10^{11}$ yr and $T_{1/2}^{isomer} = 6$ nsec, which are in reasonable agreement with experimental values[40] of $T_{1/2}^{SF} = 1.45 \times 10^{11}$ yr and $T_{1/2}^{isomer} = 3.8$ nsec. Since there are no other measured even-even fission-isomer half-lives for decay from the lowest isomeric state the values $\hbar\omega_A = 1.30$ MeV and $\hbar\omega_B = 0.60$ MeV could not be checked in this manner for other nuclei, and these values were used in all cases.

With the values for E_A, $\hbar\omega_A$, $\hbar\omega_B$, and the statistical parameters fixed from a comparison with other experimental results, the present statistical model contains only three adjustable parameters whose values may be determined from a comparison with experimental isomer excitation functions. These three independent parameters are: (1) $E_{II}(A)$, the height of the secondary minimum above the ground state which is determined from the measured isomer threshold (i.e., energy intercept); (2) $E_B(A+1) - E_{II}(A)$, which is contained in the fission-neutron competition for decay from the $(A+1)$ nucleus and determines the maximum isomer-to-prompt-fission ratio; and (3) $E_B(A) - E_{II}(A)$, which is involved in the fission γ-ray competition in the final deexcitation of states populated in the A nucleus.

C. Fits to Experimental Fission-Isomer Excitation Functions

Using three adjustable parameters $E_{II}(A)$, $E_B(A+1) - E_{II}(A)$, and $E_B(A) - E_{II}(A)$ calculations

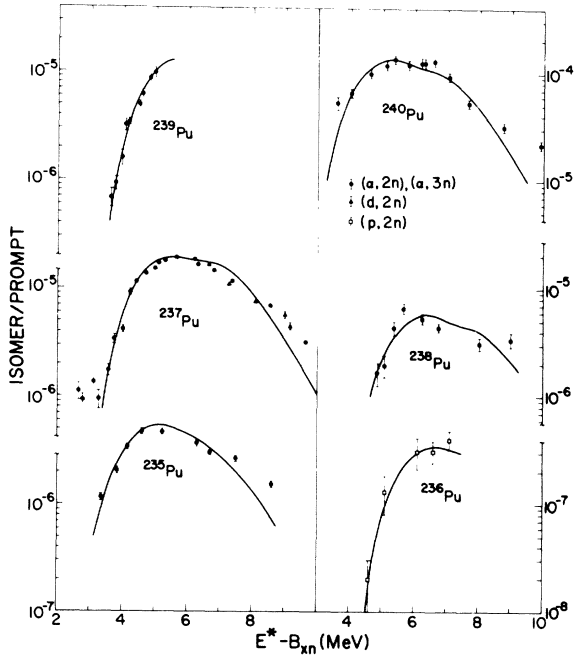

FIG. 14. Fits to experimental $(2n)$ and $(3n)$ data for production of fission isomers in various plutonium isotopes. Solid curves are calculated excitation functions obtained as described in the text. Data for ^{236}Pu were taken from Lark *et al.* (Ref. 13).

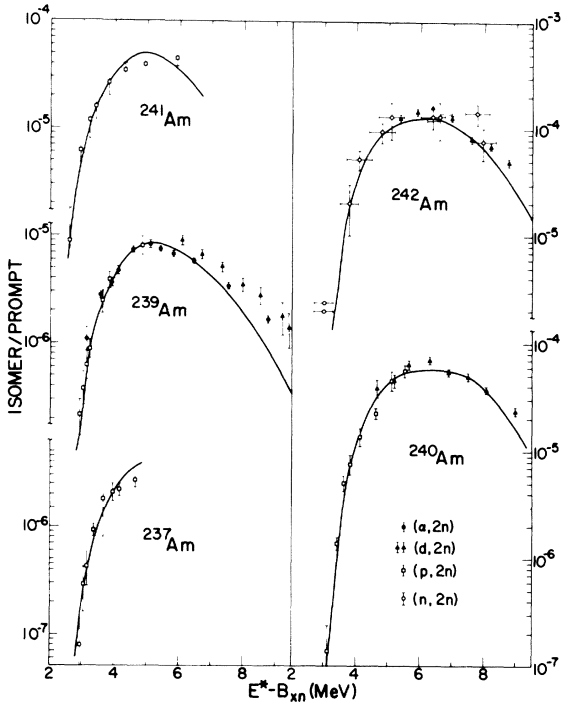

FIG. 15. Fits to experimental $(2n)$ data for production of fission isomers in various americium isotopes. Solid curves are calculated excitation functions obtained as described in the text. Open points are obtained from Refs. 11–14. For ^{239}Am the $(p,2n)$ data were multiplied by a factor of 1.3 to obtain better over-all agreement between $(p,2n)$ and $(\alpha,2n)$ results.

were performed as described in the previous sections, and fits were obtained to experimental excitation functions for forming fission isomers in various Pu, Am, and Cm isotopes. The data and fitted curves are shown in Figs. 14–16 and the fission-barrier parameters obtained from those fits are listed in Table II. The experimental data used in these fits include $(\alpha, 2n)$, $(\alpha, 3n)$, and $(d, 2n)$ results from the present experiment (solid points); $(p, 2n)$ and $(d, 2n)$ results reported by the Copenhagen group[12–14] (open points); the $(n, 2n)$ measurements of Flerov *et al.*[11]; and results from the ^{242}Pu$(\alpha, 3n)^{243m}$Cm reaction and the ^{244}Pu$(\alpha, 3n)^{245m}$Cm reaction[41] from Wolf and Unik.[29] The minimum errors (±0.2 MeV) quoted on parameters in Table II include estimates for possible errors due to uncertainties in the various fixed parameters of the statistical model (see Appendix B). The errors on the parameters do not include possible systematic changes that might occur if different level-density functions were used in well II and on top of barrier B. In cases where only the initial rise of the excitation function is measured the parameter $E_B(A) - E_{II}(A)$ could not be determined.

In addition to the excitation functions shown in Figs. 14–16, measurements have been made on the population of isomers of ^{241m}Pu, ^{240m}Am, and ^{242m}Am from the (γ, n) reaction.[20,21] The present statistical model cannot be used directly to fit these results, because of the complicated spectrum of excitation produced by the bremsstrahlung γ-ray beam. However, the authors have fitted these results with calculations based on the Jackson model[25] for neutron evaporation and they obtain apparent thresholds $E_{II} = 3.25 \pm 0.25$ MeV and $E_{II} = 3.30 \pm 0.20$ MeV for ^{240m}Am and ^{242m}Am, respectively, as compared with values of 3.0 ± 0.2 and 2.9 ± 0.2 MeV from present fits to $(2n)$ evaporation data leading to these same nuclei. These results suggest that the present model gives values for E_{II} which are ~0.3 MeV lower than obtained with analyses based on the Jackson model. A similar shift is observed between the E_{II} values in Table II and those originally deduced for $(2n)$ and $(3n)$ reactions using the Jackson model.[12–14,18] From this comparison the value $E_{II} = 2.9 \pm 0.15$ determined by Gangrsky, Markov, and Tsipenyuk[21] from ^{241}Pu has been decreased by 0.3 MeV and is listed as 2.6 ± 0.3 MeV in Table II.

As discussed previously[14,15,18] the isomers ^{236m}Pu and ^{238m}Pu appear to be anomalous in that they have thresholds 1–1.5 MeV higher than their odd-even neighbors and longer half-lives than expected. These isomers are believed to correspond to the decay of excited states in the second potential well with the lowest isomeric states decaying with a lifetime too short to be observed. The isomers observed in ^{242m}Cm and ^{244m}Cm appear to be similar and the limited data suggest a similar case for

TABLE II. Fission-barrier parameters from fits to experimental fission-isomer excitation functions. In all cases values $\hbar\omega_A = 1.3$ MeV and $\hbar\omega_B = 0.6$ MeV were used.

Nucleus	E_A[a] (MeV)	E_{II} (MeV)	$E_B(A+1) - E_{II}$ (MeV)	$E_B(A+1)$ (MeV)	$E_B(A) - E_{II}$ (MeV)	$E_B(A)$ (MeV)
^{235}Pu	5.8	2.4 ± 0.2	2.6 ± 0.2	5.0	2.6 ± 0.2	5.0
^{236}Pu	...	4.0 ± 0.3[b]	...	...	...	...
^{237}Pu	5.8	2.9 ± 0.2	2.7 ± 0.2	5.6	2.5 ± 0.2	5.4
^{238}Pu	...	3.7 ± 0.2[b]	...	...	...	...
^{239}Pu	5.8	2.6 ± 0.2	2.4 ± 0.3	5.0		
^{240}Pu	5.8	2.6 ± 0.3	2.65 ± 0.2	5.25	2.75 ± 0.2	5.35
^{241}Pu		2.6 ± 0.3[c]				
^{237}Am	6.4	2.4 ± 0.2	2.9 ± 0.4	5.3	...	...
^{238}Am	6.4	2.7 ± 0.2[d]	2.8 ± 0.3[d]	5.5	...	...
^{239}Am	6.4	2.5 ± 0.2	2.7 ± 0.2	5.2	2.7 ± 0.2	5.4
^{240}Am	6.4	3.0 ± 0.2	3.2 ± 0.2	6.2	3.05 ± 0.2	6.05
^{241}Am	6.4	2.2 ± 0.2	2.9 ± 0.2	5.1		
^{242}Am	6.4	2.9 ± 0.3	3.1 ± 0.2	6.0	3.1 ± 0.2	6.0
^{241}Cm	6.2	2.3 ± 0.2	2.4 ± 0.2	4.7	2.7 ± 0.2	5.0
^{242}Cm	...	3.2 ± 0.3[b]	...	...	...	...
^{243}Cm	6.2	2.0 ± 0.3	2.4 ± 0.3	4.4	2.8 ± 0.3	4.8
^{244}Cm	...	3.7 ± 0.3[b]	...	...	...	...
^{245}Cm	6.2	2.4 ± 0.3	2.1 ± 0.3	4.5	2.5 ± 0.3	4.9

[a] Values of E_A were determined from neutron-fission-threshold measurements as described in the text.
[b] Assumed to be thresholds for excited states in the second well (see text and Table III).
[c] Reference 21, with corrections for difference in analysis techniques (see text).
[d] Results obtained from a fit to unpublished ^{239}Pu$(p, 2n)^{238m}$Am results from G. Sletten, private communication.

^{246m}Cm. The cross sections for populating these isomers cannot be obtained from the present model. Thresholds were estimated by shifting the calculated fits for ^{240m}Pu to fit the ^{236m}Pu and ^{238m}Pu data and by shifting the calculated ^{241m}Cm fits for the ^{242m}Cm and ^{244m}Cm results. Some properties of these anomalous isomers are listed in Table III. Estimates for peak values of the ratio of isomer-to-ground-state cross sections were obtained using $\langle \Gamma_n/\Gamma_f \rangle$ systematics.[31]

Fits to experimental data with the present statistical model give values for E_{II} that are on the average about 0.3 MeV lower than those obtained using the previous constant-temperature Jackson model.[25] These results give E_{II} values about 1 MeV greater than those estimated by Jägare[26] using a similar approach. The major differences between the present statistical model and that used by Jägare is that: (1) Jägare used an unreasonably large temperature $T = 1.25$ MeV as compared to $T \sim 0.4$ MeV which has been shown by Gilbert and Cameron[33] to be appropriate for actinide nuclei at low excitations; and (2) Jägare effectively assumed that $a_f/a_n = 1.0$, whereas in the present calculations the ratio a_f/a_n was adjusted to reproduce experimental $\langle \Gamma_n/\Gamma_f \rangle$ values. The large temperature used by Jägare would tend to underestimate E_{II} values.

D. Systematics of Fission-Barrier Parameters

The fission-barrier parameters obtained from fits to experimental fission excitation functions are listed in Table II and plotted as a function of mass number in Fig. 17. The results give isomer excitation energies which are similar (~2—3 MeV) for all the Pu, Am, and Cm nuclei studied. The depths of the isomeric wells also appear similar with a slight maximum for Am nuclei and a definite decrease for Cm nuclei. In all cases the fits give $E_A > E_B$ with the largest difference $E_A - E_B \sim 1.5$ MeV occurring for Cm isotopes. As will be discussed in more detail below there are some inconsistencies in the parameters obtained and in comparison of the fission barriers determined in these experiments with those implied by other types of experiments. Thus, there may still be some systematic errors in the barrier parameters due to inadequacies in the formulation of the present statistical model for calculating fission-isomer cross sections.

The most serious internal inconsistency obtained in fitting the experimental results occurs for the

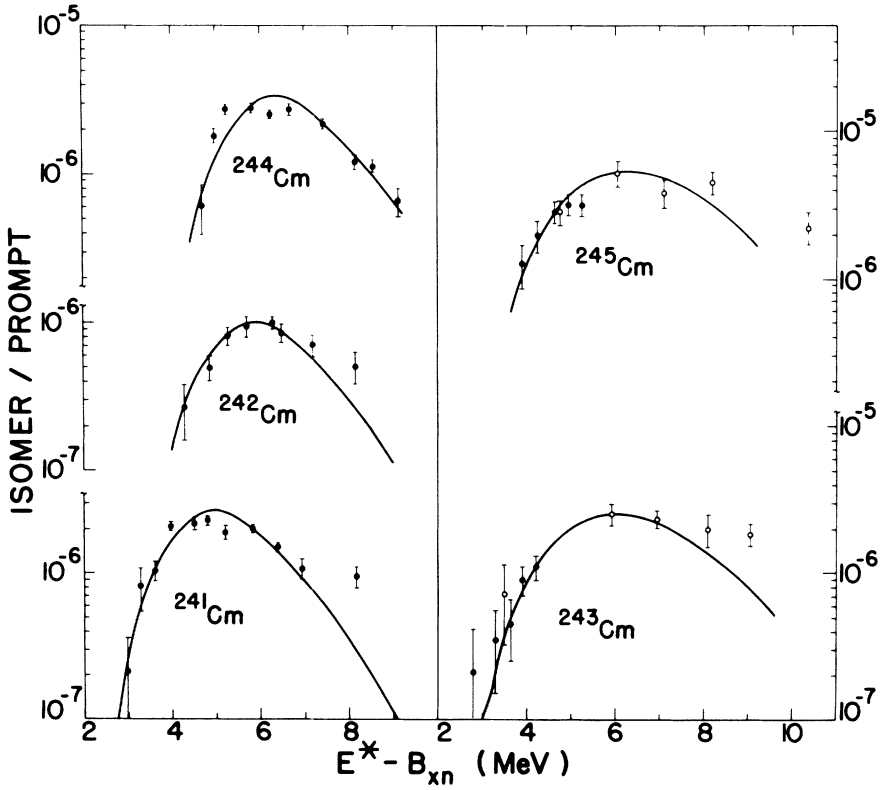

FIG. 16. Fits to experimental ($2n$) and ($3n$) data for production of fission isomers in various curium isotopes. Solid curves are calculated excitation functions obtained as described in the text. Open points are obtained from Wolf and Unik (Ref. 29). ^{245}Cm data have been renormalized as described in Ref. 41.

TABLE III. Properties of "anomalous" even-even fission isomers.

Isomeric nucleus	Z	N	$T_{1/2}$ (nsec)	E_{II} (MeV)	Peak isomer/prompt (units of 10^{-6})	Peak isomer/ground state (units of 10^{-4})
^{236m}Pu	94	142	34 ± 8 [a]	4.0 ± 0.3	0.4	0.1
^{238m}Pu	94	144	6.5 ± 1.5	3.7 ± 0.2	5	0.4
^{242m}Cm	96	146	>80	3.2 ± 0.3	1	0.1
^{244m}Cm	96	148	>100	3.7 ± 0.3	3	0.1
^{246m}Cm	96	150	...	...	<2	<0.03

[a] See Ref. 13.

Am isotopes where the data require the following characteristics in order to obtain acceptable fits: (1) E_{II} values are ~0.5 MeV greater for ^{240}Am and ^{242}Am than for neighboring odd-A isotopes, (2) $E_B - E_{II}$ is approximately independent of mass number, and (3) $E_B(A+1) - E_{II}(A) \approx E_B(A) - E_{II}(A)$. These three characteristics lead to different values of E_B deduced for a particular nucleus depending on whether it is involved in the production or decay of the isomeric states. For example, the fits give $E_B = 6.05$ MeV from the decay of ^{240}Am isomers in the fit to the ^{240m}Am excitation function and they give $E_B = 5.20$ MeV for ^{240}Am in the calculation of the formation of ^{239m}Am isomers. This inconsistency could be due to error in the Q values for the $(p, 2n)$ reactions[30] or more likely to an error in the level-density functions used in the isomer calculations. Since the level densities used in the calculations reproduce the odd-even effects for measured D_I values at the neutron binding energy and reproduce observed odd-even effects in $\langle \Gamma_n/\Gamma_f \rangle$, this discrepancy suggests that the present statistical model should be modified to allow for either: (1) an odd-even variation in the nuclear temperature used in the low-energy portion of the level-density functions, or (2) a level-density function in well II that is different from that in well I and/or a different level-density function for the calculation of Γ_B than for the calculation of Γ_A. Because ^{240}Pu is the only even-even ground-state isomer ob-

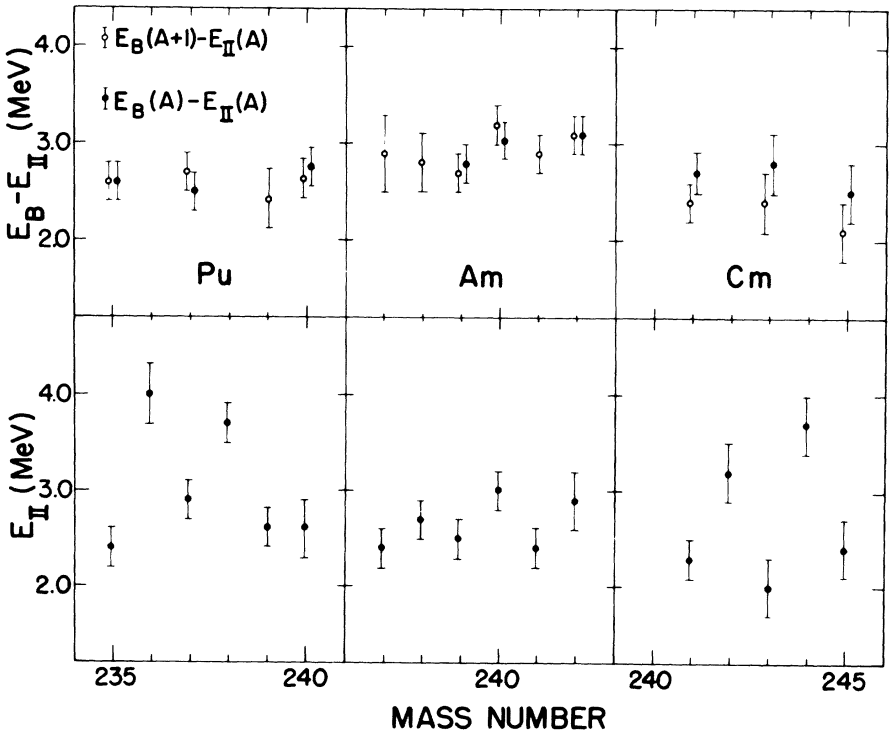

FIG. 17. Variation of the parameters E_{II}, $E_B(A+1) - E_I(A)$, and $E_B(A) - E_{II}(A)$ obtained from fits to experimental data with the statistical model as described in the text.

served and its threshold is not very well determined, it is not possible to tell whether there is an odd-even discrepancy in the fits with the present model to results for the Pu isotopes.

Another check on the barrier parameters for ^{242}Am can be obtained by comparing to the measured isomer-production cross section for the reaction ^{241}Am$(n,\gamma)^{242m}$Am. Measurements of Flerov *et al.*[6] give a value of the fraction of the neutron-capture reactions which form isomers, $\sigma_i/\sigma_{CN} \sim 0.5 \times 10^{-5}$ for neutrons in the energy region 1–2 MeV. Calculations using the present model with $E_B = 6.0$ MeV predict $\sigma_i/\sigma_T \sim 2 \times 10^{-4}$, or roughly a factor of 20 larger than measured. However, if E_B is assumed to be 5.5 MeV, then the model would predict $\sigma_i/\sigma_T \sim 2 \times 10^{-5}$, and furthermore at excitation energies of 1–2 MeV above E_B many of these nuclei might be lost to fission in a prompt (n,γ,f) reaction. Thus, this comparison also suggests that the E_B (and maybe also E_{II}) values obtained from fits to the even Am isomer data are too large.

A final check on the consistency of the present statistical model can be made by comparing calculated and experimental values for the average level spacings in the two wells. A comparison of experimental and calculated D_I and D_{II} values is given in Table IV. From Table IV it is seen that the experimental and calculated values of D_I are in reasonable agreement but there are large discrepancies between experimental and calculated values of D_{II}. From the limited data available there seems to be an odd-even dependence in the discrepancy between experimental and calculated D_{II}/D_I values. For ^{240}Pu the calculated D_{II}/D_I is about twice the experimental value but for the odd-A isotopes ^{239}Pu, ^{241}Pu, and ^{245}Cm, the calculated values of D_{II}/D_I are 5–10 times greater than measured. With the present model this discrepancy in calculated and measured D_{II}/D_I values could probably be eliminated by either: (1) using a level-density function in well II that has a different form from that used in well I; and/or modifying the low-energy dependence of the level density to allow for an odd-even dependence in the nuclear temperature.

Thus, the inconsistencies in the Am barriers, the comparison of calculated experimental (n,γ) cross sections, and the comparison of calculated and experimental D_{II}/D_I values all suggest that the level-density function in the second well (and maybe on top of barrier B) should be modified. In all of the presently available cases the experimental results relevant to level densities in the first well $[D_I(B_n)$, and $\langle \Gamma_n/\Gamma_f \rangle_{av}]$ sample primarily the properties of the level density at energies greater than ~4 MeV where the Gilbert and Cameron prescription[33] gives a level-density function $\rho(E) \propto e^{2\sqrt{aU}}$. Experimental results appropriate to the second well $[D_{II}(B_n)$ and isomer-production cross sections] sample primarily the properties of the level density for energies less than ~3 MeV where Gilbert and Cameron prescribe a level density $\rho(E) \propto e^{(E-E_0)/T}$. Because different regions of the level density are sampled in the different processes, it is difficult to determine whether the discrepancies described above are due to a faulty description of the low-energy portion of the level-density function or whether the assumption that the same form of level-density function can be used in the two wells is not valid. Further theoretical guidance on the dependence of the nuclear level density as a function of deformation is needed before much more progress can be made in the detailed interpretation of phenomena associated with fission through a two-peaked barrier.

TABLE IV. Comparison of calculated and experimental level spacings in the two potential wells for angular momentum states appropriate for the neutron-capture reactions.

Compound nucleus	J	D_I Calc. (eV)	D_I Expt. (eV)	D_{II} Calc. (eV)	D_{II} Expt. (eV)	D_{II}/D_I Calc.	D_{II}/D_I Expt.
^{239}Pu	$\frac{1}{2}^+$	4.3	13 [a]	1700	1000 [a]	400	80
^{240}Pu	1^+	1.5	3 [a]	500	460 [a]	360	150
^{241}Pu	$\frac{1}{2}^+$	12	14 [a]	6000 [b]	700 [a]	500	50
^{242}Am	$2^-, 3^-$	0.26	0.56 [a]	...	...	...	...
^{245}Cm	$\frac{1}{2}^+$	11	14 [c]	2700	1000 [c]	250	70

[a] Reference 32.
[b] For $E_{II} = 2.6$ MeV from Ref. 21, with corrections for difference in analysis techniques.
[c] Reference 38.

E. Comparison of Experimental and Theoretical Fission-Barrier Parameters

There have been attempts by several groups to calculate the shape of fission barriers for actinide

TABLE V. Comparison of experimental and theoretical fission-barrier parameters for ^{240}Pu. Energies are measured relative to ground-state energy.

	Experimental results	Theoretical results Pauli *et al.* (Ref. 44)	Theoretical results Nix *et al.* (Ref. 45)
E_A	5.8 [a]	5.2	5.8
E_{II}	2.6 ± 0.3	2.3	2.7
E_B	5.35 ± 0.2	5.5	5.6

[a] Average value for plutonium isotopes obtained from measurements of neutron-induced-fission cross sections as described in the text.

nuclei using the general approach of making single-particle corrections to a liquid-drop mass surface. The early calculations[3,42] allowed only symmetric shapes for the nucleus and it was found that the results generally overestimated the height of the second barrier relative to the first barrier. Recently calculations by Möller and Nilsson[43] have shown that in the vicinity of the second barrier the nucleus is unstable toward reflection-asymmetric shapes and when these shapes were allowed in the calculations the predicted height of the second barrier is lowered substantially. Detailed calculations allowing asymmetric shapes in the region of the second barrier have been performed for ^{240}Pu by Pauli, Ledergerber, and Brack[44] and by Nix *et al.*[45] and the results of their calculations are compared with the present experimental results in Table V. It is seen that there is remarkable agreement for ^{240}Pu between the present experimental barrier parameters obtained using the statistical model described above and results of theoretical calculations.

ACKNOWLEDGMENTS

We gratefully acknowledge the help of Neil Lark in the initial setup and planning for these experiments. We are indebted to J. R. Nix and S. Bjørnholm for many interesting and stimulating discussions. We would like to thank G. Sletten, K. L. Wolf, and J. P. Unik for allowing us to use their data before publication. Most of the targets were prepared by Judith Gursky and J. G. Povelites. The ^{244}Pu was supplied by D. Hoffman and the target was prepared by W. A. Sedlacek.

APPENDIX A

Level-Width Expressions

Standard statistical theory allows us to write expressions for the widths involved in our model (or more strictly to the transmission factors that are proportional to the ratios of width to level spacing) that are dependent almost entirely on the parameters of the chosen level-density expression.

We outline first the neutron-width expressions. In reaction theory the width for neutron decay through a single channel with given channel spin s, and orbital angular momentum l from a state with total angular momentum and parity J^{π} to a state of the residual nucleus A, Z with angular momentum and parity $I^{\pi'}$ is normally expressed as the product of a penetration factor through the centrifugal barrier P_l and a reduced width $\gamma^2_{J(n'sl)}$ [i.e., $\Gamma_{J(n'sl)} = 2P_l\gamma^2_{J(n'sl)}$]. The penetration factor depends on the neutron wave number k and the effective nuclear-force radius R,

$$P_l = \frac{kR}{j_l^2(kR) + n_l^2(kR)}, \tag{A1}$$

where j_l and n_l are the spherical Bessel and Neumann functions.

The reduced width is a much more complicated quantity but the simple expression from the "strong-coupling" model is probably as good an expression for its gross average behavior as any. This is

$$\frac{\gamma^2(n')}{D} = \frac{1}{\pi KR}, \tag{A2}$$

where K is a measure of the wave number of a "single-particle" neutron inside the nucleus. To evaluate this numerically, the nucleus is assumed to have a well depth of approximately 48 MeV, and the nuclear-force radius R is taken to be $R = 1.35\ A^{1/3}$ fm. The total neutron width that we require for the isomer-decay calculations is the sum of the individual widths over all final states of the residual nucleus and all spin and orbital angular momentum channels. In statistical theory the sum over final states is replaced by an integral over level density of the residual nucleus. Thus,

$$\frac{\Gamma_{J(n)}}{D_{J\pi}} = \sum_I \sum_{s=|I-\frac{1}{2}|}^{I+\frac{1}{2}} \sum_{l=|J-s|}^{J+s} \int_0^{E-S_n} \frac{2}{\pi KR}\, d\epsilon \times \rho(A, Z, \epsilon, I, \pi' = \pi(-1)^l) P_l(kR). \tag{A3}$$

In this expression k is computed for the neutron energy $E - S_n - \epsilon$, ϵ being the excitation energy of the residual nucleus. This is the expression calculated in our computer program, the limitation on the sum over I being governed effectively either by the spin attenuation factor in the level-density law or by the negligibly small values of the penetration factor for high l. In principle, different level-density laws should be used for the calculations of neutron widths to class-I and class-II shapes of the residual nucleus. In our calculations the same level-density law is used. Equation (A3) is hence the expression for the class-I neutron width; the expression for the class-II-state neutron width is obtained simply by replacing the neutron separation energy S_n by its sum with the isomer excitation energy E_{II}.

In our model of shape-isomer excitation, radiation widths concerns us only for the residual nucleus A, Z. Here we make the standard assumptions of statistical theory that only electric dipole transitions are significant and that the radiation widths for individual transitions are proportional only to the phase-space factor $\epsilon_\gamma{}^3$. The total radiation

width is then given by

$$\frac{\Gamma_{J^\pi(\gamma f)}}{D_{J^\pi}} = C \sum_{J_f=|J-1|}^{J+1} \int_0^E d\epsilon\, \rho(A, Z, \epsilon, I, \pi' = \pi)(E-\epsilon)^3 \tag{A4}$$

for states with excitation energy E. This again is the expression for class-I states. That for class-II states is obtained by replacing E by $E - E_{II}$. The proportionality constant C for Eq. (A4) is obtained by requiring the expression to give the observed total radiation widths for the slow-neutron resonances.

The expressions for transitions across the deformation barriers, A and B, are taken from the original Bohr-Wheeler expression for fission widths across a single barrier,

$$\frac{\Gamma_{(F)}}{D} = \frac{N}{2\pi}, \tag{A5}$$

where N is the number of states of internal excitation of the system that are energetically available at the barrier. This expression was extended to near-barrier energies by Hill and Wheeler who included a Gamow type of tunneling factor, which, for an inverted-harmonic-oscillator (with circular frequency ω) form of barrier, can be shown to be

$$T_f(E) = 1 + e^{2\pi(E_f - E)/\hbar\omega} \tag{A6}$$

for each internal state with energy E_f (with respect to the normal ground state of the nucleus). With this extension the total fission width (of the decaying nucleus $A+1$, Z) becomes

$$\frac{\Gamma_{J^\pi(F)}}{D_{J^\pi}} = \frac{1}{2\pi} \int_0^\infty dE_f \frac{\rho(A+1, Z, J, E_f - V, \pi)}{1 + e^{2\pi(E_f - E)/\hbar\omega}} . \tag{A7}$$

Provided that $2\pi/\hbar\omega$ is rather greater than the reciprocal of the effective temperature corresponding to the level-density law at $E - V$, the integrand of this expression has an exponential attenuation for $E_f > E$. The integral, in fact, is not expected to be very sensitive to the value of $\hbar\omega$ except at low energies. The widths for barrier transitions $\Gamma_{(A)}$ and $\Gamma_{(B)}$ are obtained from Eq. (A7) simply by substituting the barrier heights E_A or E_B for V, and tunneling parameters $\hbar\omega_A$ and $\hbar\omega_B$ for $\hbar\omega$.

APPENDIX B

1. Determination of Nuclear Level Density

The formalism of Gilbert and Cameron[33] was chosen for determining the level densities needed in the calculation of the various decay widths. This formalism includes the effects of both pairing and ground-state shell corrections on the level density. The parameters for the stable deformation have been deduced[33] by comparison with a variety of experimental data for nuclei throughout the periodic table.

The level-density formulas used are:

for $E < E_x$,

$$\rho_1(E, J) = \frac{1}{T} e^{(E - E_0)/T} \frac{(2J+1)\exp[-(J+\frac{1}{2})^2/2\sigma^2]}{2\sigma^2} ; \tag{B1}$$

for $E > E_x$,

$$\rho_2(E, J) = \frac{\sqrt{\pi}}{12} \frac{e^{2\sqrt{aU}}}{a^{1/4}U^{5/4}} \frac{(2J+1)\exp[-(J+\frac{1}{2})^2/2\sigma^2]}{2\sqrt{2\pi}\,\sigma^3} ; \tag{B2}$$

where $U = E - P(Z) - P(N)$ and $P(Z)$, $P(N)$ are empirical pairing corrections determined by Gilbert and Cameron.[33] The matching energy E_x was taken from the systematics of Gilbert and Cameron as

$$E_x = 3.13 + P(Z) + P(N) \text{ MeV} .$$

The spin-cutoff factor σ was taken equal to 5.45 MeV for all cases. For a particular value of the "level-density" parameter a in ρ_2, the values of E_0 and T in the expression for ρ were determined by requiring that ρ_1 and ρ_2 be matched in value and first derivative at the transition energy E_x.

In the model proposed by Gilbert and Cameron, the level-density parameter a is a function of the shell correction

$$a/A = 0.009\,17S + 0.120 , \tag{B3}$$

where $S = S(Z) + S(N)$ are shell corrections determined empirically from comparison with experimental data. In this model it is natural to let a be a function of deformation, since the two-peaked fission barrier is created by the variation in the shell correction with deformation. At the two minima in the potential surface the value of S is a minimum and consequently a should have a minimum value. For lack of evidence to the contrary the present calculations assume $a_n = a_I = a_{II}$. At the tops of the two maxima in the fission barrier the values of S are at maxima and again for lack of information to the contrary it is assumed that $a_f = a_A = a_B$.

Values for a_n were obtained from Gilbert and Cameron[33] with average values of S used for all isotopes of the same element. Similarly average values of the total pairing energy were used. Then the values of a_f were determined by comparing calculations of the average values $\langle \Gamma_n/\Gamma_f \rangle$ with previous compilations[31] of experimental results. The actual parameters used in the calculations are given in Table VI. These parameters are in reasonable agreement with results from heavy-ion reactions[46] which indicated that $a_f/a_n = 1.2 \pm 0.1$.

TABLE VI. Statistical parameters used in level-density calculations.

	Pu isotopes	Am isotopes	Cm isotopes
$a_{I,II}$	26.5 MeV^{-1}	26.2 MeV^{-1}	25.5 MeV^{-1}
a_f	28.5 MeV^{-1}	32.0 MeV^{-1}	32.0 MeV^{-1}
$T_{I,II}$	0.411 MeV	0.414 MeV	0.421 MeV
T_f	0.394 MeV	0.368 MeV	0.367 MeV
Pairing E	0.61, 1.11 MeV [a]	0.0, 0.48 MeV [a]	0.72, 1.16 MeV [a]

[a] Values for odd- and even-neutron isotopes, respectively.

Calculated values of Γ_n/Γ_f are compared with experimental results and the empirical systematics (solid line) of Vandenbosch and Huizenga[31] in Fig. 18. The results show that using the parameters in Table V and V_A values discussed in Sec. IV B, the calculated values of Γ_n/Γ_f for an energy of 4 MeV above the neutron binding energy are in reasonable agreement with experimental results. However, for plutonium isotopes the calculations give an increase of a factor of ~1.5–2 when the equivalent neutron energy is increased from 4 to 10 MeV, while for curium isotopes Γ_n/Γ_f is seen to decrease by a factor of ~2–3 for this change in energy. This dependence is contrary to experimental evidence which suggests that Γ_n/Γ_f varies less rapidly with excitation energy. Another way to compare the calculations with experimental results is to compare directly to the spallation cross-section measurements which were used to derive the Γ_n/Γ_f values shown in Fig. 18. A comparison to experimental spallation data[47-50] for various cases is shown in Fig. 19. The results in Fig. 19 show that the present model gives a reasonable representation of data in the energy region where the $2n$ reaction is dominant. However, the calculated % spallation drops much more rapidly than experimental results when the $(3n)$ reaction starts to come in. This discrepancy is because the calculated Γ_n/Γ_f values are varying too rapidly with energy. This comparison suggests that putting in a simple variation of a with deformation may not give an adequate description of the change in the level-density function with deformation. A level-density function where a is a function of energy may give a better representation[51] of the effect of shell corrections on the nuclear level density and such a function would tend to give better agreement between calculated and experimental $\langle \Gamma_n/\Gamma_f \rangle$ values. For the curium isotopes the comparisons in Figs. 18 and 19 suggest that the present average parameter set gives too large an odd-even fluctuation in the calculated values of Γ_n/Γ_f. In principle the values of a_f determined in these comparisons could be converted to shell-correction energies via Eq. (B3) above and then compared to theoretical calculations of shell corrections. At pres-

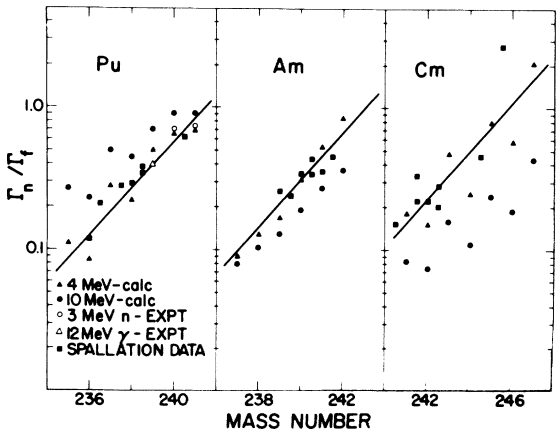

FIG. 18. Comparison of calculated and experimental average values for Γ_n/Γ_f for plutonium, americium, and curium isotopes. Experimental values and the solid line are taken from the compilation of Vandenbosch and Huizenga (Ref. 31).

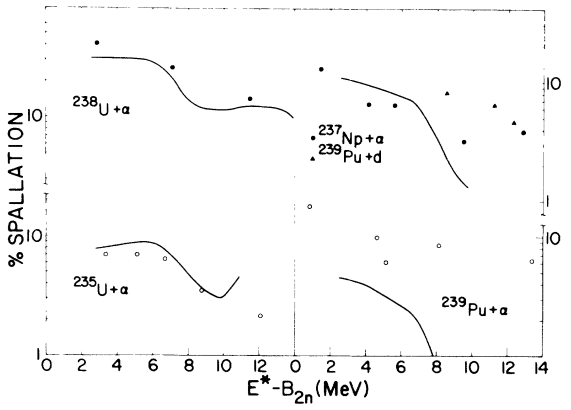

FIG. 19. Comparison of calculated and experimental measurements of the percent of the total compound-nucleus-formation cross section going into $(2n)$ and $(3n)$ spallation reactions. Experimental results are obtained from the following sources: $\alpha + ^{235}$U – Vandenbosch *et al.* (Ref. 47); $\alpha + ^{238}$U – Wing *et al.* (Ref. 48); $\alpha + ^{239}$Pu – Glass *et al.* (Ref. 49); and $\alpha + ^{237}$Np, $d + ^{239}$Pu – Gibson (Ref. 50).

ent it is believed that the model being used for level-density calculations is too crude to allow much meaning to be attached to such a comparison.

2. Sensitivity of Statistical-Model Calculations to Various Parameters and Assumptions

The calculations plotted in Figs. 20 and 21 indicate the sensitivity of the isomer calculations, based on the present statistical model, to all of the important parameters involved in this model. Figure 20 shows variations of parameters around the best-fit values for the population of the fission isomer in ^{240}Pu by the $2n$ reaction.

Figure 20(a) shows the two components which contribute to production of the fission isomer. At energies near threshold the cross section is dominated by direct evaporation to the isomeric shape and subsequent γ-ray emission (P_{22}). At high energies the process is dominated by evaporation to a highly excited state in the first well followed by penetration of barrier A and subsequent γ-ray emission (P_{21}). As described in Sec. IV A3 the low-energy side of the P_{21} contribution is sensitive to assumptions about the degree of coupling between class-I and class-II states and in the actual calculations a sharp cutoff was used at the energy where the width of states in the second well was equal to the spacing of levels in the first well ($\Gamma_B = D_1$). Figure 20(d) shows that changing this assumption over wide limits has little effect on the calculated curves. The high-energy slope of P_{21} is sensitive to the sharp-cutoff assumption that in the second well the (γ, f) decay process dominates for $E^* > E_B + 1.0$ MeV. If a more realistic smooth-cutoff approximation is used (or if more than one step of the γ-ray deexcitation process were included in the calculations) better agreement between calculated and experimental slopes for the high-energy portion of the excitation functions could probably be obtained. In addition, some of the events in the high-energy tail may cor-

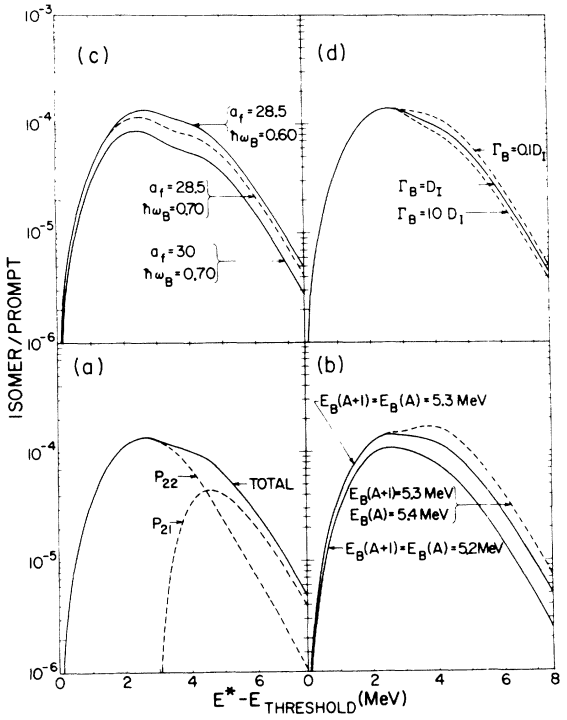

FIG. 20. Sensitivity of the isomer-excitation-function calculations to various parameters in the statistical model for the reaction ^{238}U$(\alpha, 2n)^{240m}$Pu. In part (a) the two components P_{22} and P_{21} come from direct population of states in the second well and population of isomeric states by penetration of barrier A and subsequent γ-ray deexcitation, respectively. In part (d) the effect of changing the low-energy cutoff in the decay calculation from the excitation energy corresponding to $\Gamma_B = 10 D_1$ to the excitation energy corresponding to $\Gamma_B = 0.1 D_1$ is illustrated.

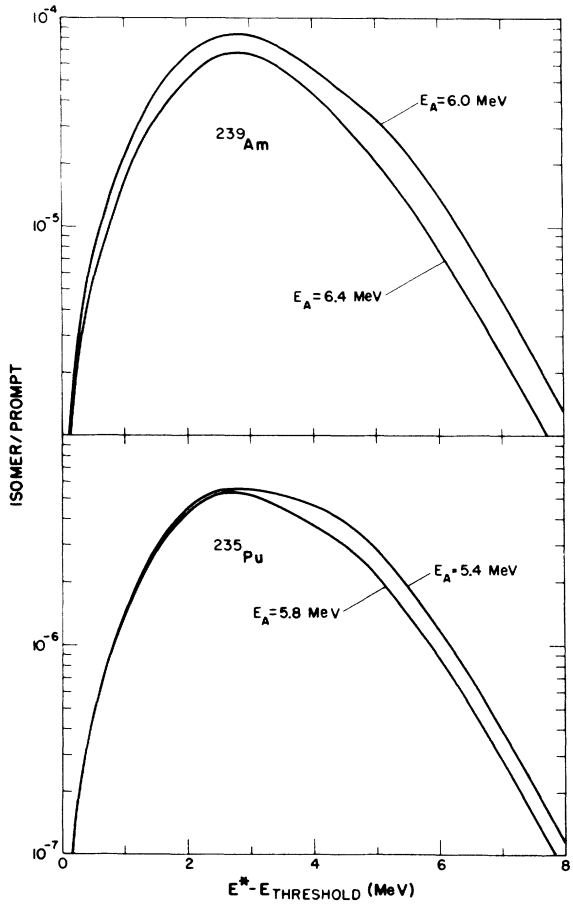

FIG. 21. Sensitivity of the isomer-excitation-function calculations to change in E_A for the population of fission isomers in ^{235}Pu and ^{239}Am.

respond to events involving a direct neutron-knockout reaction followed by the subsequent evaporation of one or more neutrons. This type of reaction is not taken into account in the present model.

Figure 20(b) shows that variation of the major parameters of the model, $E_B(A+1)$ and $E_B(A)$, by 0.1 MeV gives a change of 20–30% in the calculated isomer cross sections. Figure 20(c) shows that variations of a_f and $\hbar\omega_B$ within reasonable limits do not have dramatically large effects on the calculated isomer cross sections. It has recently been shown[52] that the odd-even variations in isomer and ground-state half-lives can be correlated with a possible odd-even variation in $\hbar\omega$ (i.e., a variation in the effective mass for penetration of the fission barrier). Introduction of these $\hbar\omega$ values[52] into the present calculations produce systematic changes in the fitted E_B values of the order of 0.1 MeV.

The sensitivity of the calculated cross sections to E_A is dependent on the absolute value of Γ_n/Γ_f. Figure 21 shows that for one of the least fissionable cases (^{239}Am) a change of 0.4 MeV in E_A for both ^{240}Am and ^{239}Am is roughly equivalent to a change of ~0.05 MeV in E_B [see Fig. 20(B)], while for a very fissionable nucleus (^{235}Pu) a change of 0.4 MeV in E_A for both ^{236}Pu and ^{235}Pu has a much smaller effect on the calculated isomer cross section.

An assumption of the present model is that the decay of states in the second well is governed only by the penetrability of the barrier B and the level spacing D_{II}. Below the top of barrier B it is known that the fission strength is concentrated in narrow vibrational resonances so that at energies removed from these resonances decay by fission is probably further inhibited by the weakness of the coupling between the fission vibrations and the compound levels. The practical importance of this effect in the present model is dependent on how far below the top of barrier B the penetrabilities allow competition from fission decay. To test this sensitivity the ^{239m}Am and ^{240m}Am data were refit with a modified model which assumed that for energies less than $E_B - 0.5$ MeV the nucleus was caught in the second well and could not decay by fission. When equivalent fits were obtained to the experimental data it was found that this "sharp-cutoff" model gave the same fitted values for $E_B(A+1)$ and gave values for $E_B(A)$ which were 0.2 and 0.1 MeV lower than originally obtained for ^{239}Am and ^{240}Am, respectively. From this comparison it is concluded that the strong-coupling assumption used in calculating the fission decay from well II does not have a serious effect on the values obtained for E_B from fits to the experimental data.

---

*Work performed under the auspices of the U.S. Atomic Energy Commission.

†Visiting staff member from Atomic Energy Research Establishment, Harwell, England.

[1]S. M. Polikanov, V. A. Druin, V. A. Karnaukhov, V. L. Mikheev, A. A. Pleve, N. K. Skobelev, V. G. Subbotin, G. M. Ter-Akop'yan, and V. A. Fomichev, Zh. Eksperim. i Teor. Fiz. 42, 1464 (1962) [transl.: Soviet Phys. – JETP 15, 1016 (1962)].

[2]A review of the early work is given in S. M. Polikanov, Usp. Fiz. Nauk, 94, 43 (1968) [transl.: Soviet Phys.–Usp. 11, 22 (1968)].

[3]V. M. Strutinski, Nucl. Phys. A95, 420 (1967); A122, 1 (1968); S. Bjørnholm and V. M. Strutinski, *ibid.* A136, 1 (1969).

[4]A. Fubini, J. Blons, A. Michaudon, and D. Paya, Phys. Rev. Letters 20, 1373 (1968).

[5]E. Migneco and J. P. Theobald, Nucl. Phys. A112, 603 (1968).

[6]G. N. Flerov, A. A. Pleve, S. M. Polikanov, S. P. Tretyakova, I. Boca, M. Sezon, I. Vilcov, and N. Vilcov, Nucl. Phys. A102, 443 (1967).

[7]I. Boca, N. Martalogu, M. Sezon, I. Vilcov, G. N. Flerov, A. A. Pleve, S. M. Polikanov, and S. P. Tretyakova, Nucl. Phys. A134, 541 (1969).

[8]Yu. P. Gangrsky, K. A. Gavrilov, B. N. Markov, N. C. Khanh, and S. M. Polikanov, Yadern. Fiz. 10, 65 (1969) [transl.: Soviet J. Nucl. Phys. 10, 38 (1970)].

[9]B. Dalhsuren, G. N. Flerov, Yu. P. Gangrskyo, Yu. P. Lasarev, B. N. Markov, and N. C. Khanh, Nucl. Phys. A148, 337 (1970).

[10]A. J. Elwyn and A. T. G. Ferguson, Nucl. Phys. A148, 337 (1970).

[11]G. N. Flerov, A. A. Pleve, S. M. Polikanov, S. P. Tretyakova, N. Martalogu, D. Poenaru, M. Sezon, I. Vilcov, and N. Vilcov, Nucl. Phys. A97, 444 (1967).

[12]S. Bjørnholm, J. Borggreen, L. Westgaard, and V. A. Karnaukhov, Nucl. Phys. A95, 513 (1967).

[13]N. L. Lark, G. Sletten, J. Pedersen, and S. Bjørnholm, Nucl. Phys. A139, 481 (1969).

[14]S. M. Polikanov and G. Sletten, Nucl. Phys. A151, 656 (1970).

[15]R. Vanderbosch and K. L. Wolf, in *Proceedings of the Second International Atomic Energy Symposium on Physics and Chemistry of Fission, Vienna, Austria, 1969* (International Atomic Energy Agency, Vienna, Austria, 1969), p. 439.

[16]V. Metag, R. Repnow, P. von Brentano, and J. D. Fox, in *Proceedings of the Second International Atomic Energy Symposium on Physics and Chemistry of Fission, Vienna, Austria, 1969* (see Ref. 15), p. 449; R. Repnow, V. Metag, and P. von Brentano, to be published.

[17]J. B. Natowitz and J. K. Archer, Phys. Letters 30B, 469 (1969).

[18]S. C. Burnett, H. C. Britt, B. H. Erkkila, and W. E. Stein, Phys. Letters 31B, 523 (1970).

[19]P. A. Russo, R. Vandenbosch, M. Mehta, J. R. Tesmer, and K. L. Wolf, Phys. Rev. C 3, 1595 (1971).

[20]Yu. P. Gangrsky, B. N. Markov, and Yu. M. Tsipenyuk, Yadern. Fiz. 11, 54 (1970) [transl.: Soviet J. Nucl. Phys. 11, 30 (1970)].

[21]Yu. P. Gangrsky, B. N. Markov, and Yu. M. Tsipenyuk, Phys. Letters 32B, 182 (1970).

[22]S. Bjørnholm, I. Broggreen, Yu. P. Gangrsky, and G. Sletten, Yadern. Fiz. 8, 459 (1968) [transl.: Soviet J. Nucl. Phys. 8, 267 (1969)].

[23]R. Repnow, V. Metag, J. D. Fox, and P. von Brentano, Nucl. Phys. A147, 183 (1970).

[24]K. L. Wolf, R. Vandenbosch, P. A. Russo, M. K. Mehta, and C. R. Rudy, Phys. Rev. C 1, 2096 (1970).

[25]J. D. Jackson, Can. J. Phys. 34, 767 (1956).

[26]S. Jägare, Nucl. Phys. A137, 241 (1969); Phys. Letters 32B, 571 (1970).

[27]H. Jungclaussen, Yadern. Fiz. 7, 83 (1968) [transl.: Soviet J. Nucl. Phys. 7, 60 (1968)].

[28]D. R. F. Cochran, private communication.

[29]K. L. Wolf and J. P. Unik, Bull. Am. Phys. Soc. 16, 55 (1971).

[30]A. H. Wapstra, C. Kurzeck, and A. Anisinoff, in *Proceedings of the Third International Conference on Atomic Masses, Winnipeg, Canada, 1968*, edited by R. C. Barber (University of Manitoba Press, Winnipeg, Canada, 1968), p. 622.

[31]R. Vandenbosch and J. R. Huizenga, in *Proceedings of the Second United Nations International Conference on the Peaceful Uses of Atomic Energy, Geneva, 1958* (United Nations, Geneva, Switzerland, 1958), Vol. 15, p. 284; see also E. K. Hyde, I. Perlman, and G. T. Seaborg, *The Nuclear Properties of the Heavy Elements* (Prentice-Hall, Inc., Englewood Cliffs, New Jersey, 1964), Vol. III, p. 307 ff.

[32]J. E. Lynn, in *Proceedings of the Second International Atomic Energy Symposium on Physics and Chemistry of Fission, Vienna, Austria, 1969* (see Ref. 15), p. 249.

[33]A. Gilbert and A. G. W. Cameron, Can. J. Phys. 43, 1446 (1965).

[34]H. C. Britt and J. D. Cramer, Phys. Rev. C 2, 1758 (1970).

[35]G. F. Auchampaugh, private communication.

[36]C. D. Bowman, G. F. Auchampaugh, S. C. Fultz, and R. W. Hoff, Phys. Rev. 166, 1219 (1968).

[37]*Neutron Cross Sections*, compiled by J. R. Stehn, M. D. Goldberg, R. Wiener-Chasman, S. F. Mughabghab, B. A. Magurno, and V. M. May, Brookhaven National Laboratory Report No. BNL-325 (U.S. GPO, Washington, D.C., 1965), 2nd ed., Suppl. 2, Vol. II, $Z = 88$ to 98.

[38]M. S. Moore and G. A. Keyworth, Phys. Rev. C 3, 1656 (1971).

[39]J. D. Cramer and J. R. Nix, Phys. Rev. C 2, 1048 (1970).

[40]L. Z. Malkin *et al.*, At. Energ. (USSR) 15, 158 (1963) [transl.: Soviet J. At. Energy 15, 851 (1964)].

[41]A comparison of data from the ^{244}Pu$(\alpha, 3n)^{245m}$Cm reaction indicated a discrepancy of ~50% between cross sections obtained by Wolf and Unik (Ref. 29) and those reported in this paper. In the present experiments the ^{244}Pu target was very thin and throughout most of the measurements had a large crack in the center. In this one case a significant fraction of the isomers formed could have been lost by recoiling out of the target. Consequently the ^{245m}Cm isomer/prompt ratios were multiplied by a factor of 1.5 to give better agreement with the results of Wolf and Unik. Also some of the discrepancy would be eliminated if the shorter half-life reported by Wolf and Unik were used in analyzing the present data.

[42]S. G. Nilsson, C. F. Tsang, A. Sobiczewski, Z. Szymanski, S. Wycech, C. Gustafsson, I. L. Lamm, P. Möller, and B. Nilsson, Nucl. Phys. A131, 1 (1969).

[43]P. Möller and S. G. Nilsson, Phys. Letters 31B, 283 (1970).

[44]H. C. Pauli, T. Ledergerber, and M. Brack, Phys. Letters 34B, 264 (1971); and private communication.

[45]J. R. Nix, M. Bolsterli, E. O. Fiset, and J. Norton, to be published.

[46]T. Sikkeland, J. E. Clarkson, N. H. Steiger-Shafrir, and V. E. Viola, Phys. Rev. C 3, 329 (1971).

[47]R. Vandenbosch, T. D. Thomas, S. E. Vandenbosch, R. A. Glass, and G. T. Seaborg, Phys. Rev. 111, 1358 (1958).

[48]J. Wing, W. J. Ramler, A. L. Harkness, and J. R. Huizenga, Phys. Rev. 114, 163 (1959).

[49]R. A. Glass, R. J. Carr, J. W. Cobble, and G. T. Seaborg, Phys. Rev. 104, 434 (1956).

[50]W. M. Gibson, University of California Radiation Laboratory Report No. UCRL-3493, 1956 (unpublished).

[51]V. S. Ramamurthy, S. S. Kapoor, and S. K. Kataria, Phys. Rev. Letters 25, 386 (1970).

[52]B. B. Back, J. P. Bondorf, G. A. Otroschenko, J. Pedersen, and B. Rasmussen, Nucl. Phys. A165, 449 (1971).